

Prepared in the fall of 1994 for the proceedings of the
19th International Nathiagali Summer College on Physics and Contemporary Needs, Nathiagali 1994
edited by S. A. Ahmad and S. M. Farooqi
(should have been published by Pak Book Company, but did never appear in print)

ELEMENTS OF MICROMASER PHYSICS

Berthold–Georg Englert

*Sektion Physik, Universität München
Am Coulombwall 1, D-85748 Garching^a*

Abstract

The elements of micromaser physics are reviewed in a tutorial way. The emphasis is on the basic theoretical concepts, not on technical details or experimental subtleties. After a brief treatment of the atom-photon interaction according to the Jaynes-Cummings model, the master equation that governs the dynamics of the one-atom maser is derived. Then the more important properties of the steady states of the one-atom maser are discussed, including the trapped states. The approximations, upon which the standard theoretical model of the one-atom maser is based, are exhibited. The methods by which one calculates statistical properties of the emerging atoms are hinted at.

This is a tutorial review of micromaser physics, mainly from the point of view of a theoretician. The audience aimed at consists of non-experts who want to get an idea about this field of research without perhaps having the time to go into the finer details. More technical reviews are, of course, available in the published literature. I would like to draw special attention to the recent articles of the Garching group [1] and of the Paris group [2], which are both contained in an up-to-date collection of essays on cavity quantum electrodynamics [3]. In these articles, the reader will find very many references to papers on various subtle aspects of micromaser physics that are well beyond the scope of this tutorial review. There are also textbooks on quantum optics [4] that devote some space to a treatment of the micromaser. Some more recent work that is not included in these reviews or textbooks will be cited in the text.

^aAlso at Max-Planck-Institut für Quantenoptik, Hans-Kopfermann-Straße 1, D-85748 Garching.

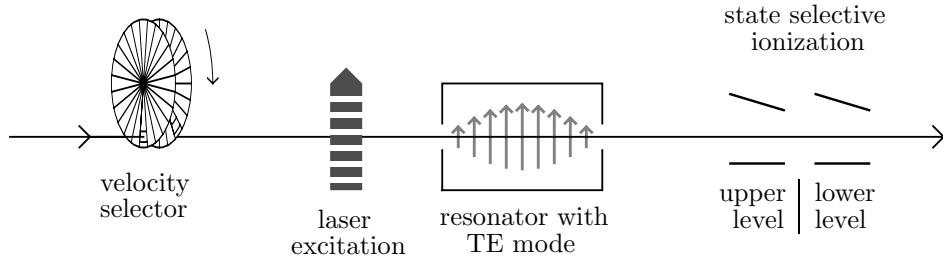


FIG. 1: Schematic setup of micromaser experiments.

Experimental setup and other introductory remarks

The most important parts of the setup of a micromaser experiment are sketched in Fig. 1. A beam of neutral alkaline atoms (rubidium is the most popular species) is run through a resonator, which has a very large quality factor to ensure a long photon lifetime. The high quality is achieved by superconducting surfaces, for which purpose the resonator is made of niobium and cooled below the critical temperature of 4.2 K. This low temperature has the additional benefit that the number of thermal photons is very small (remember the Planck radiation) and thus the thermal noise is reduced.

The resonator is tuned such that it possesses a mode in the microwave regime (of TE type in Fig. 1) which is resonant with an atomic transition between two Rydberg levels. It is this privileged mode that we shall be interested in exclusively. The frequencies of all other resonator modes are very far away on the scale set by the linewidth of the privileged mode, which is extremely narrow owing to the high resonator quality.

We refer to said atomic transition between the two distinguished Rydberg states as the masing transition. Prior to entering the resonator the atoms are excited to (one of) these Rydberg states. Transitions between Rydberg states with principal quantum numbers in the 50s to 70s are in the convenient microwave range, where resonators of ultrahigh quality are available. In addition, Rydberg atoms are very large (diameters of a few thousand Ångström units are typical) and therefore possess enormous dipole moments, so that a strong coupling of the atom to the photons in the privileged mode is achieved. It is then possible that the atoms emit microwave photons with a large probability. Since the photons are stored for a rather

long time in the resonator — lifetimes of a considerable fraction of a second have been realized experimentally — even a faint beam of atoms can pump the resonator effectively. In this way, a maser is operated in which single atoms traversing the resonator provide for an efficient pump. One is then dealing with a microscopic maser indeed, a *micromaser*.

The excitation of the atoms to the Rydberg states of interest is typically achieved by a laser beam which is crossed by the atoms cross just before they enter the resonator. It is advantageous to select a narrow velocity group in the atom beam because then all atoms interact for the same well-controlled time with the resonator photons. A velocity selection can be performed with the aid of a set of Fizeau wheels, as indicated in Fig. 1, or by other means (see the more technical review articles).

The high quality of the resonator is quite essential for all micromaser experiments. Therefore one cannot perform any direct measurements on the stored photon field. The only information available is the state of the emerging atoms. Ideally they can solely end up in either one of the states of the masing transition. The atoms are probed by state selective ionization in inhomogeneous electric fields, symbolically indicated in Fig. 1 by two pairs of nonparallel condensor plates. At the first stage only atoms in the upper masing level are ionized, in the second stage only those in the lower level. The stripped-off electrons are detected and thus the final state of the atom is determined.

The levels of the ^{85}Rb isotope that are most relevant for many of the micromaser experiments in Garching are depicted in Fig. 2. As indicated, the masing levels will be called α and β throughout. In this figure, the excitation from the ground state to the state α is shown as a one-step process. That can be done by a suitably tuned, frequency doubled, ring dye laser. But different excitation schemes, that involve intermediate levels, have also been used successfully.

The heart of the experiment is the interaction of the excited atom with the resonator photons. To a reasonably good approximation only the two Rydberg levels of the masing transition are significant for the dynamics during the passage of the atom through the resonator. We shall, therefore, simplify matters and think of the masing atoms as two-level systems. The state vectors $|\rightarrow\rangle \equiv |\alpha\rangle$ and $|\leftarrow\rangle \equiv |\beta\rangle$, respectively, are then used to denote the excited and the deexcited state of such a two-level atom.

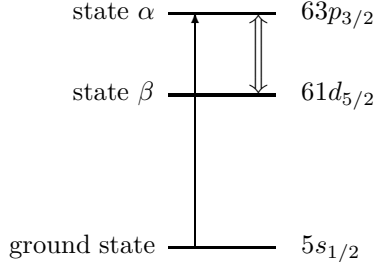


FIG. 2: Levels of ^{85}Rb relevant for some of the Garching micromaser experiments. The laser excitation from the ground state to the upper masing level α is indicated by the \uparrow arrow, the masing transition by the \updownarrow arrow. The level spacing is not drawn to scale.

Atom-photon interaction (Jaynes-Cummings model)

A symbolic representation of the passage of a two-level atom through the resonator is shown in Fig. 3. Initially the atom is in state α and there are supposedly n photons in the resonator, so that the initial state vector of the combined atom-field system is $|\alpha, n\rangle = |\uparrow, n\rangle$. After the interaction we may have either one of two final state vectors — $|\alpha, n\rangle$ if no photon has been emitted, or $|\beta, n+1\rangle = |\downarrow, n+1\rangle$ if a photon has been emitted — or a superposition of both.

For a calculation of the actual final state we use the standard *Jaynes-Cummings model*¹ for the theoretical description of the atom-field dynamics. The fundamental variables of the privileged field mode are the photon ladder operators a and a^\dagger with their well known properties, of which

$$\begin{aligned}
 [a, a^\dagger] = 1, \quad a^\dagger a |n\rangle &= |n\rangle n \\
 a^\dagger |n\rangle &= |n+1\rangle \sqrt{n+1}
 \end{aligned}
 \tag{1}$$

are perhaps the most important ones. Likewise we employ ladder operators σ and σ^\dagger for the two-level atoms. Their defining properties are

$$\begin{aligned}
 \sigma |\alpha\rangle &= |\beta\rangle \quad \text{or} \quad \sigma |\uparrow\rangle = |\downarrow\rangle, \\
 \sigma^\dagger |\beta\rangle &= |\alpha\rangle \quad \text{or} \quad \sigma^\dagger |\downarrow\rangle = |\uparrow\rangle,
 \end{aligned}
 \tag{2}$$

¹The name derives from a 1963 paper [5].

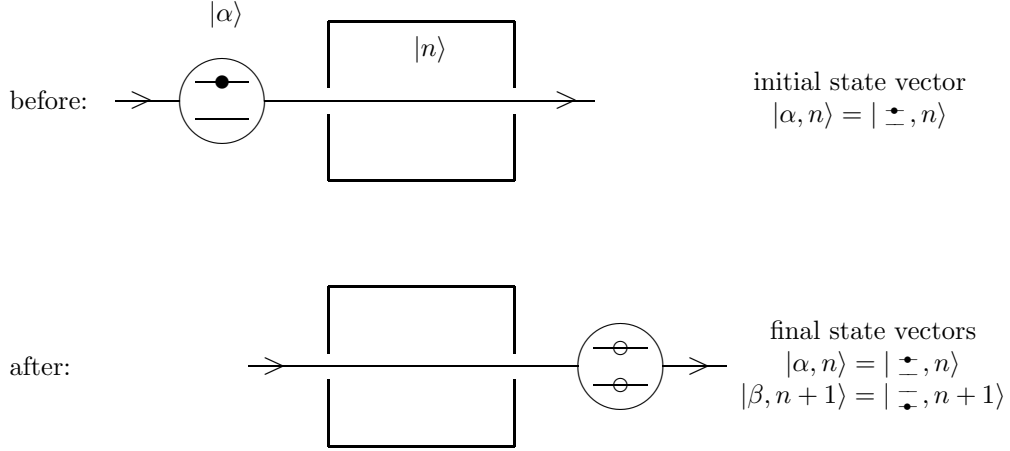


FIG. 3: Before and after the passage of a two-level atom that is initially excited through a resonator with n photons initially. _____

and

$$\begin{aligned} \sigma |\beta\rangle &= 0 \quad \text{or} \quad \sigma |\downarrow\rangle = 0, \\ \sigma^\dagger |\alpha\rangle &= 0 \quad \text{or} \quad \sigma^\dagger |\uparrow\rangle = 0, \end{aligned} \quad (3)$$

with the consequences

$$\sigma^2 = 0, \quad \sigma^{\dagger 2} = 0 \quad (4)$$

as well as

$$\begin{aligned} \sigma^\dagger \sigma &= |\alpha\rangle \langle \alpha| = |\uparrow\rangle \langle \uparrow|, \\ \sigma \sigma^\dagger &= |\beta\rangle \langle \beta| = |\downarrow\rangle \langle \downarrow|. \end{aligned} \quad (5)$$

The latter are useful ways of expressing the projectors to the atomic states.

In the Jaynes-Cummings model the dynamics is generated by the Hamiltonian operator

$$H = \underbrace{\hbar\omega a^\dagger a}_{\text{photon}} + \underbrace{\hbar\Omega \sigma^\dagger \sigma}_{\text{atom}} - \underbrace{\hbar g(t)(a^\dagger \sigma + \sigma^\dagger a)}_{\text{interaction}}. \quad (6)$$

Here, $\hbar\omega$ is the energy per photon, $\hbar\Omega$ is the atomic level spacing (the de-excited atom is assigned energy zero by convenient convention), and the so-called Rabi frequency $g(t)$ measures the strength of the interaction. Inasmuch

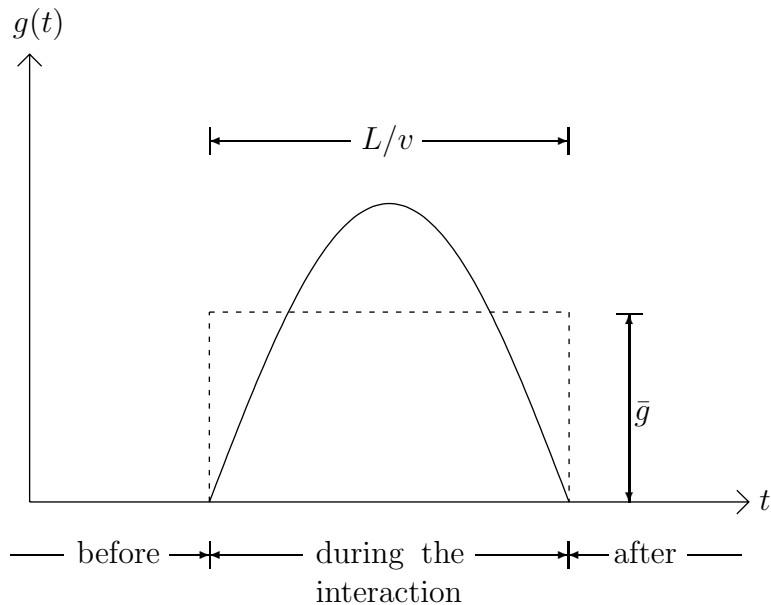


FIG. 4: Time dependent Rabi frequency $g(t)$ (solid line) and effective Rabi frequency \bar{g} .

as the atom enters and leaves the resonator, this Rabi frequency possesses a natural time dependence. It vanishes as long as the atom is outside the resonator, and is large while the atom is inside. To the extent to which the atomic center-of-mass motion is classical,² the duration of the interaction is given by the ratio L/v of the cavity length L and the atomic velocity v . These circumstances are sketched in Fig. 4 where we also indicate the effective Rabi frequency \bar{g} , which is given by the time average of $g(t)$,

$$\bar{g} = \frac{v}{L} \int dt g(t). \quad (7)$$

To be specific let us report typical numbers for the micromaser experiments in Garching that make use of the Rydberg transition of Fig. 2. The resonator is

²This condition is very well obeyed under the ordinary experimental conditions. Under extreme circumstances, however, the quantum nature of the center-of-mass motion may become important [6].

of cylindrical shape with an almost circular cross section of diameter ~ 24 mm and a length L that is also ~ 24 mm. The experiments use the photons in the TE_{121} mode. Here one has the frequency values

$$\begin{aligned}\omega &\cong \Omega \cong 2\pi \times 21.5 \text{ GHz}, \\ \bar{g} &\cong 44 \text{ kHz} = \pi \times 14 \text{ kHz},\end{aligned}\tag{8}$$

which correspond to the energy values

$$\begin{aligned}\hbar\omega &\cong \hbar\Omega \cong 9 \times 10^{-5} \text{ eV}, \\ \hbar\bar{g} &\cong 3 \times 10^{-11} \text{ eV}.\end{aligned}\tag{9}$$

Please note how small is the energy per photon³ and how tiny is the interaction energy.

The transition operator

$$\gamma \equiv a^\dagger \sigma + \sigma^\dagger a\tag{10}$$

affects atomic transitions along with the emission or absorption of a photon:

$$\begin{aligned}\gamma |\pm, n\rangle &= |\mp, n+1\rangle \sqrt{n+1}, \\ \gamma |\mp, n+1\rangle &= |\pm, n\rangle \sqrt{n+1}.\end{aligned}\tag{11}$$

The eigenvalues of γ are $\gamma' = 0, \pm 1 \pm \sqrt{2}, \pm\sqrt{3} \dots$, and its eigenstates (so-called ‘dressed states’ of one kind in the jargon of quantum optics) are very simple linear combination of the atom-field states that we have been using so far, viz.

$$\begin{aligned}|\gamma_0\rangle &\equiv |\mp, 0\rangle, & |\gamma_n^\pm\rangle &\equiv \frac{1}{\sqrt{2}} (|\pm, n\rangle \pm |\mp, n+1\rangle), \\ \gamma |\gamma_0\rangle &= 0, & \gamma |\gamma_n^\pm\rangle &= |\gamma_n^\pm\rangle (\pm\sqrt{n+1}).\end{aligned}\tag{12}$$

They are mutually orthogonal and normalized to unity,

$$\langle \gamma' | \gamma'' \rangle = \delta(\gamma', \gamma'') = \begin{cases} 1 & \text{if } \gamma' = \gamma'' \\ 0 & \text{if } \gamma' \neq \gamma'' \end{cases}\tag{13}$$

³Recall that visible photons have energies of 1–2 eV.

and complete,

$$\sum_{\gamma'} |\gamma'\rangle \langle \gamma'| = 1, \quad (14)$$

and constitute a convenient basis for expanding arbitrary state vectors.

The important identity

$$\gamma^2 = a^\dagger a + \sigma^\dagger \sigma \quad (15)$$

is easily demonstrated with the aid of the algebraic properties of the ladder operators stated in Eqs. (1)–(5). We use it to rewrite the Hamilton operator (6) into a form,

$$H = \hbar\omega\gamma^2 + \hbar(\Omega - \omega)\sigma^\dagger\sigma - \hbar g(t)\gamma, \quad (16)$$

which is particularly transparent on resonance ($\omega = \Omega$):

$$H(t) = \hbar\omega\gamma^2 - \hbar g(t)\gamma. \quad (17)$$

For the sake of simplicity, we shall confine ourselves to this resonant situation for the rest of this tutorial review.

Since the transition operator is then a constant of motion — the vanishing commutator $[H(t), \gamma(t)] = 0$ implies $\gamma(t) = \gamma(t_0)$ — the Schrödinger equation obeyed by the eigenstates of $\gamma(t)$ is very simple. For the left eigenstates, it reads

$$i\hbar \frac{\partial}{\partial t} \langle \gamma', t | = \langle \gamma', t | H(t) = [\hbar\omega\gamma'^2 - \hbar g(t)\gamma'] \langle \gamma', t |. \quad (18)$$

and can be solved immediately. The outcome is

$$\langle \gamma', t | = \underbrace{\exp[-i\omega\gamma'^2(t - t_0)]}_{\text{free evolution}} \underbrace{\exp\left[i\gamma' \int_{t_0}^t dt' g(t')\right]}_{\text{interaction}} \langle \gamma', t_0 |. \quad (19)$$

We note that the evolution is naturally split into two contributions: the free evolution and what results from the interaction.

We are particularly interested in the overall change asked for in the context of Fig. 3. Then the instants t_0 and t are ‘before’ and ‘after’ the interaction, so that the integral in (19) equals the effective Rabi frequency of (7) times the classical interaction time L/v ,

$$\int_{t_0}^t dt' g(t') = \bar{g}L/v \equiv \varphi. \quad (20)$$

For obvious reasons, the quantity φ here introduced is called the accumulated Rabi angle. This single number summarizes the net effect of the atom-field interaction.

We have thus found a first central result of micromaser theory:

Resonant interaction leads to a change

$$\begin{aligned} \langle \gamma' | &\rightarrow e^{i\varphi\gamma'} \langle \gamma' | \\ | \gamma' \rangle &\rightarrow | \gamma' \rangle e^{-i\varphi\gamma'} \end{aligned} \quad (21)$$

on top of the free evolution.

As an application let us reconsider the situation of Fig. 3. First, we write the initial state vector $|\pm, n\rangle$ as a superposition of eigenvectors of the interaction operator γ ,

$$\begin{aligned} |\pm, n\rangle &= \frac{1}{2} (|\pm, n\rangle + |\mp, n+1\rangle) + \frac{1}{2} (|\pm, n\rangle - |\mp, n+1\rangle) \\ &= \frac{1}{\sqrt{2}} (|\gamma_n^+\rangle + |\gamma_n^-\rangle). \end{aligned} \quad (22)$$

Second, we make use of (21) to find the change resulting from the interaction,

$$|\pm, n\rangle \xrightarrow{\text{interaction}} \frac{1}{\sqrt{2}} \left[|\gamma_n^+\rangle \exp(-i\varphi\sqrt{n+1}) + |\gamma_n^-\rangle \exp(i\varphi\sqrt{n+1}) \right]. \quad (23)$$

Third, we express the outcome in terms of the atom-field states,

$$|\pm, n\rangle \xrightarrow{\text{interaction}} |\pm, n\rangle \cos(\varphi\sqrt{n+1}) + |\mp, n+1\rangle [-i \sin(\varphi\sqrt{n+1})], \quad (24)$$

which is the desired result. In particular, it states the probabilities with which the two possible final atom-field states occur,

$$|\pm, n\rangle \xrightarrow{\text{interaction}} \begin{cases} |\pm, n\rangle & \text{with probability } \cos^2(\varphi\sqrt{n+1}), \\ |\mp, n+1\rangle & \text{with probability } \sin^2(\varphi\sqrt{n+1}). \end{cases} \quad (25)$$

It is essential to realize that this result is dramatically different from the one in the usual spontaneous-and-induced emission process. There the

physics is well described by the lowest-order perturbation theory, in which the argument $\varphi\sqrt{n+1}$ of the sine and cosine function in (25) is infinitesimal and individual transitions are not happening frequently. In addition, usual spontaneous emission involves not only just one mode of the radiation field but a continuous range of modes with neighboring frequencies. In summary, the photon emission in a micromaser experiment has nothing in common with the much more familiar spontaneous emission by atoms in free space.

We note that there are special situations in which the photon emission happens with certainty,

$$|\uparrow, n\rangle \xrightarrow{\text{interaction}} |\downarrow, n+1\rangle \quad \text{if } \varphi\sqrt{n+1} = \pi/2 \quad (26)$$

(e. g. $n = 0$, $\varphi = \pi/2$),

or in which surely no emission takes place,

$$|\uparrow, n\rangle \xrightarrow{\text{interaction}} |\uparrow, n\rangle \quad \text{if } \varphi\sqrt{n+1} = \pi \quad (27)$$

(e. g. $n = 0$, $\varphi = \pi$).

Of course, one could add integer multiples to $\varphi\sqrt{n+1}$ in both cases without changing the final states. Clearly, these special situations are unknown in the context of the usual spontaneous emission. In the micromaser the atom can first emit and then reabsorb the photon — this is the case of (27) — thus undergoing a complete Rabi cycle, or perhaps a few complete cycles.

One-atom operation

The beam of atoms in Fig. 1 comes originally from an opening in an oven, has been collimated, and perhaps velocity selected, before it is directed through the resonator. If no special action is taken, as is the standard experimental situation, the atoms in the beam are uncorrelated. In other words, the atoms arrive at random. The probability $p(t)dt$ that two successive atoms are separated in time by $t \cdots t + dt$ is thus given by the Poisson formula⁴

$$p(t)dt = e^{-rt}r dt, \quad (28)$$

⁴The Poisson formula governs also more mundane phenomena, such as the temporal spacing between drops of rain.

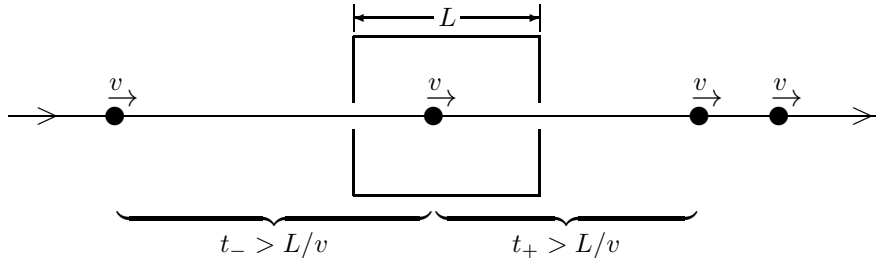


FIG. 5: An atom gives rise to a one-atom event if the temporal separations from its predecessor, t_+ , and from its successor, t_- , both exceed the classical interaction time L/v , equal to the ratio of the cavity length L and the atomic velocity v . —

where r is the rate at which the atoms arrive. The average temporal spacing between atoms is clearly equal to $1/r$; the average spatial distance is then v/r if all atoms move at the same speed v , a condition that we shall assume to be obeyed for the time being.

If the beam is faint enough, most of the atoms will enter the resonator after the preceding atom has left it, and will leave before the succeeding atom arrives. This is the situation depicted in Fig. 5. The probability that the middle atom in this figure gives rise to such a one-atom event is equal to the product of the probabilities that both spacings, t_- and t_+ , exceed the classical interaction time L/v . Now, the Poisson statistics (28) imply that the probability for a spacing greater than a certain specified period T is given by

$$\int_T^\infty dt p(t) = e^{-rT}. \quad (29)$$

Consequently, the asked-for probability of a one-atom event is

$$\underbrace{\exp(-rL/v)}_{t_- > L/v} \times \underbrace{\exp(-rL/v)}_{t_+ > L/v} = \exp(-2rL/v). \quad (30)$$

A typical number for L/v is $50 \mu\text{s}$, so that at the rather large beam rate of $r \cong 1000/\text{s}$ this probability is about $\exp(-0.1) \cong 90\%$. In other words, 90% of the atoms would contribute to one-atom events. More typical is a beam rate of $r \cong 10/\text{s}$, for which the probability for one-atom events is about $\exp(-0.001) = 99.9\%$. Collective events, in which more than one atom

interact with the resonator photons at the same time, are then extremely rare and can be justifiably disregarded. We are then dealing with the *One-Atom Maser*, the most intriguing version of the micromaser.

One-atom maser: Dynamics

For the theoretical treatment of the dynamics of the photon field in the one-atom maser (OAM) we employ the standard master equation approach. It deals with a coarse grain time evolution of the photon field. Changes in the field that occur on the short time scale, on which the atom-field interaction happens, are ignored. In essence, one is only interested in the changes that occur in the photon state during the passage of a fair number of atoms.

Since we are focussing on the state of the photon field, rather than on the state of the entire system consisting of very many atoms and the photon field, we are treating a partial system. More precisely: we are treating an open, driven quantum system. Its state cannot be described in terms of a state vector $|\rangle$ or (one of) its wavefunctions. What one needs is a state operator ρ , which is a positive operator of unit trace. These two properties of ρ ensure that all probabilities $\langle |\rho| \rangle$ are non-negative and that the sum of all probabilities of a complete set of mutually exclusive alternatives is unity.

The matrix elements of ρ make up the so-called density matrix; for instance, when the photon number states $\langle n|$ and $|m\rangle$ are used, we get the number-state density matrix $\rho_{nm} = \langle n|\rho|m\rangle$. Just like there are very many wavefunctions to one state vector $|\rangle$, there are also very many density matrices to one state operator ρ . It is clearly advantageous to concentrate on the (somewhat abstract) state operator in the first place, and to choose a convenient matrix representation later when it is really needed.

For the photon field inside the resonator of a OAM, the state operator ρ — we shall frequently speak of ‘the state ρ ’ simply — is a time-dependent function of the ladder operators a^\dagger and a : $\rho = \rho_t(a^\dagger, a)$. For the benefit of more transparent equations, we shall suppress the arguments of ρ where misunderstandings are unlikely. The master equation obeyed by ρ has the general structure

$$\frac{\partial}{\partial t}\rho = \frac{\partial}{\partial t}\rho|_{\text{free}} + \frac{\partial}{\partial t}\rho|_{\text{gain}} + \frac{\partial}{\partial t}\rho|_{\text{loss}}. \quad (31)$$

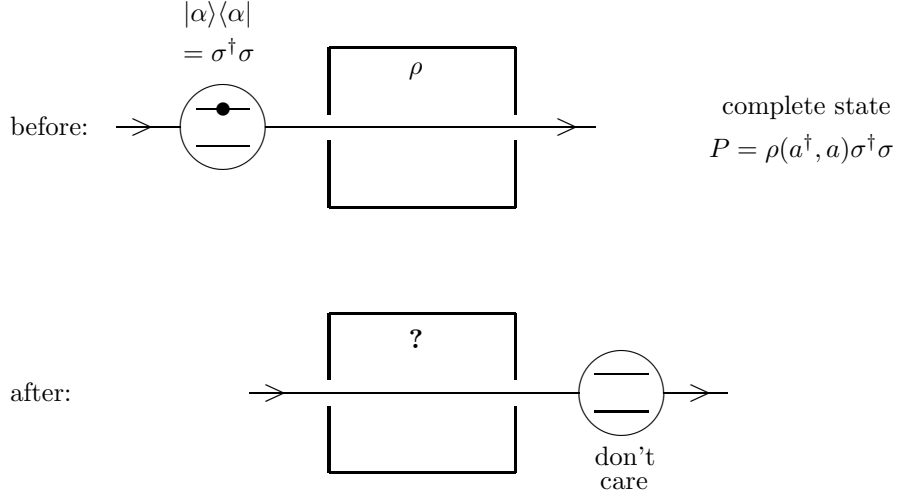


FIG. 6: Gain in OAM operation. The two-level atom is excited when it enters the resonator; the initial atomic state is $|\uparrow\rangle\langle\uparrow| = |\alpha\rangle\langle\alpha| = \sigma^\dagger\sigma$. Prior to the interaction the photon field is in the state $\rho(a^\dagger, a)$. Thus the initial state of the complete system is $P = \rho(a^\dagger, a)\sigma^\dagger\sigma$. The interaction changes this state. We do not care about the final atomic state, but want to know the photon state after the interaction.

The ‘free’ contribution is, of course, generated by the photon part of the Hamilton operator (6),

$$\left. \frac{\partial}{\partial t} \rho \right|_{\text{free}} = \frac{1}{i\hbar} [H_{\text{photon}}, \rho] = -i\omega [a^\dagger a, \rho]. \quad (32)$$

The ‘gain’ contribution to (31) is the additional change resulting from the interacting atoms traversing the resonator, and the ‘loss’ contribution originates in the coupling of the photons to their surroundings. We shall first derive the gain term and then turn to the loss term.

The gain is determined by considering the situation of Fig. 6. After employing the number-state matrix of the initial field state ρ ,

$$\rho(a^\dagger, a) = \sum_{n,m=0}^{\infty} |n\rangle \rho_{nm} \langle m|, \quad (33)$$

to write the complete initial state P in the form⁵

$$P = \sum_{n,m} |\underline{\pm}, n\rangle \rho_{nm} \langle \underline{\pm}, m| . \quad (34)$$

Now we can make use of Eq. (24) to find the effect of the interaction,

$$\begin{aligned} P \xrightarrow{\text{interaction}} & \sum_{n,m} \left[|\underline{\pm}, n\rangle \cos(\varphi\sqrt{n+1}) - |\underline{\mp}, n+1\rangle i \sin(\varphi\sqrt{n+1}) \right] \rho_{nm} \\ & \times \left[\cos(\varphi\sqrt{m+1}) \langle \underline{\pm}, m| + i \sin(\varphi\sqrt{m+1}) \langle \underline{\mp}, m+1| \right] \\ & \equiv P_{\text{after}} . \end{aligned} \quad (35)$$

This is the final state operator of the complete system consisting of one atom and the photon field (we remember that the ‘free’ evolution comes on top). We do not care about the atom and therefore we trace over the two-level degree of freedom (symbolically: tr_{atom}) to obtain the final photon state,

$$\rho(a^\dagger, a) \xrightarrow{\text{interaction}} \text{tr}_{\text{atom}} \{ P_{\text{after}} \} . \quad (36)$$

In more detail this reads

$$\begin{aligned} \rho &= \sum_{n,m} |n\rangle \rho_{nm} \langle m| \\ & \xrightarrow{\text{interaction}} \sum_{n,m} \left[|n\rangle \cos(\varphi\sqrt{n+1}) \rho_{nm} \cos(\varphi\sqrt{m+1}) \langle m| \right. \\ & \quad \left. + |n+1\rangle \sin(\varphi\sqrt{n+1}) \rho_{nm} \sin(\varphi\sqrt{m+1}) \langle m+1| \right] . \end{aligned} \quad (37)$$

Upon recalling that $a^\dagger(aa^\dagger)^{-1/2}$ is a normalized ladder operator,

$$a^\dagger(aa^\dagger)^{-1/2} |n\rangle = |n+1\rangle , \quad (38)$$

one establishes the identities

$$\begin{aligned} |n\rangle \cos(\varphi\sqrt{n+1}) &= \cos[\varphi(aa^\dagger)^{1/2}] |n\rangle , \\ |n+1\rangle \sin(\varphi\sqrt{n+1}) &= a^\dagger \frac{\sin[\varphi(aa^\dagger)^{1/2}]}{(aa^\dagger)^{1/2}} |n\rangle . \end{aligned} \quad (39)$$

⁵The letter P is a capital ρ , not a capital p .

These are then used to arrive at a second central result of micromaser theory:

Resonant interaction of atoms entering in
the \rightleftharpoons state leads to a change

$$\rho \longrightarrow \begin{aligned} & \cos[\varphi(aa^\dagger)^{1/2}] \rho \cos[\varphi(aa^\dagger)^{1/2}] \\ & + a^\dagger \frac{\sin[\varphi(aa^\dagger)^{1/2}]}{(aa^\dagger)^{1/2}} \rho \frac{\sin[\varphi(aa^\dagger)^{1/2}]}{(aa^\dagger)^{1/2}} a \end{aligned} \quad (40)$$

in the photon state on top of the free evolution.

We add the remark that an analogous result with a^\dagger and a interchanged is found for atoms that enter the resonator in the \leftarrow state. The derivation is left to the reader as a simple exercise.

The gain term in (31) is now available. It is given by

$$\begin{aligned} \left. \frac{\partial}{\partial t} \rho \right|_{\text{gain}} &= [\text{beam rate}] \times [\text{change by one atom}] \\ &= r \left\{ \cos[\varphi(aa^\dagger)^{1/2}] \rho \cos[\varphi(aa^\dagger)^{1/2}] \right. \\ & \quad \left. + a^\dagger \frac{\sin[\varphi(aa^\dagger)^{1/2}]}{(aa^\dagger)^{1/2}} \rho \frac{\sin[\varphi(aa^\dagger)^{1/2}]}{(aa^\dagger)^{1/2}} a - \rho \right\}. \end{aligned} \quad (41)$$

This expression is valid for the coarse grain time scale provided that the arriving atoms are uncorrelated, as we have assumed in Eq. (28), for example.

We turn to the loss term. Here we have to model the coupling to a thermal reservoir. In view of what we have at hand, the simplest model is that of a thermal beam of very many, very weakly interacting atoms. This beam is supposed to be at a certain temperature, so that the rate r_α of \rightleftharpoons atoms is larger than the rate r_β of the \leftarrow atoms. The ratio of these partial rates is, of course, given by the Boltzmann factor,

$$r_\alpha/r_\beta = \exp\left(-\frac{\hbar\omega}{k_B T}\right) \equiv \frac{\nu}{\nu+1}, \quad (42)$$

where k_B is the Boltzmann constant and T the temperature. Anticipating its convenience, we introduce the parametrization in terms of the positive number ν whose physical significance will become clear later.

For the \rightleftharpoons atoms in the beam, we have a contribution to the loss term which is analogous to the right-hand side of Eq. (41), except that we are now dealing with a tiny Rabi angle ϕ rather than with the macroscopic angle φ . The lowest non-vanishing order in ϕ is all that we are going to take into account. Thus we find

$$\left. \frac{\partial}{\partial t} \rho \right|_{\text{loss}, \alpha} = r_\alpha \phi^2 \left[a^\dagger \rho a - \frac{1}{2} a a^\dagger \rho - \frac{1}{2} \rho a a^\dagger \right] \quad (43)$$

for the \rightleftharpoons contribution. The \leftarrow contribution is immediately available too, because the remark after (40) implies that we have to interchange the ladder operators a and a^\dagger ,

$$\left. \frac{\partial}{\partial t} \rho \right|_{\text{loss}, \beta} = r_\beta \phi^2 \left[a \rho a^\dagger - \frac{1}{2} a^\dagger a \rho - \frac{1}{2} \rho a^\dagger a \right]. \quad (44)$$

Upon introducing the loss rate $A \equiv (r_\beta - r_\alpha) \phi^2$ and the parameter ν of (42) we combine these partial answers into

$$\begin{aligned} \left. \frac{\partial}{\partial t} \rho \right|_{\text{loss}} &= -\frac{1}{2} A (\nu + 1) \left[a^\dagger a \rho - 2 a \rho a^\dagger + \rho a^\dagger a \right] \\ &\quad - \frac{1}{2} A \nu \left[a a^\dagger \rho - 2 a^\dagger \rho a + \rho a a^\dagger \right]. \end{aligned} \quad (45)$$

The three ingredients of the master equation (31) are now at hand.

The physical significance of the rate A and the number ν is revealed by a quick look at the dynamics of an unpumped resonator, for which

$$\begin{aligned} \left. \frac{\partial}{\partial t} \rho \right|_{\text{loss}} &= -i\omega [a^\dagger a, \rho] - \frac{1}{2} A (\nu + 1) \left[a^\dagger a \rho - 2 a \rho a^\dagger + \rho a^\dagger a \right] \\ &\quad - \frac{1}{2} A \nu \left[a a^\dagger \rho - 2 a^\dagger \rho a + \rho a a^\dagger \right] \end{aligned} \quad (46)$$

is the equation of motion. This master equation is in fact so simple that the general solution for an arbitrary initial state can be written down in a number of ways. In the present context that is not so essential. We are content with these observations:

- (i) The stationary state of (46) is the thermal photon state

$$\rho_{\text{th}} = \frac{1}{\nu + 1} \left(\frac{\nu}{\nu + 1} \right)^{a^\dagger a} = \left[1 - \exp \left(-\frac{\hbar\omega}{k_B T} \right) \right] \exp \left(-\frac{\hbar\omega}{k_B T} a^\dagger a \right), \quad (47)$$

which identifies ν as the number of thermal photons inside the resonator at temperature T .

- (ii) For the evolution of the mean photon field $\langle a \rangle = \text{tr}\{a\rho\}$ (where $\text{tr} \equiv \text{tr}_{\text{photon}}$ for short) we have

$$\frac{d}{dt}\langle a \rangle = \text{tr} \left\{ a \frac{\partial}{\partial t} \rho \right\} = (-i\omega - A/2)\langle a \rangle, \quad (48)$$

so that

$$\langle a \rangle_t = \langle a \rangle_0 e^{-i\omega t} e^{-At/2}. \quad (49)$$

This shows that the field decays with the rate $A/2$ towards its stationary null value.

- (iii) Likewise we find for the mean number of photons,

$$\frac{d}{dt}\langle a^\dagger a \rangle = \text{tr} \left\{ a^\dagger a \frac{\partial}{\partial t} \rho \right\} = -A(\langle a^\dagger a \rangle - \nu), \quad (50)$$

and therefore

$$\langle a^\dagger a \rangle_t = \nu + (\langle a^\dagger a \rangle_0 - \nu)e^{-At}. \quad (51)$$

The mean photon number decays with rate A towards its stationary value of ν .

Thus the meaning of A and ν is quite clear.

The relation between the temperature of the resonator and the number of thermal photons deserves a little attention. With the numbers of Eqs. (8) and (9) we find the entries in this table:

T	ν	remarks
1.5 K	1.96	early experiments
0.5 K	0.15	typical values
80 mK	2.5×10^{-6}	achieved

Please observe that in the microwave domain thermal photons are usually present in considerable amounts. This situation is quite different from that of the optical domain in which thermal photons are irrelevant.

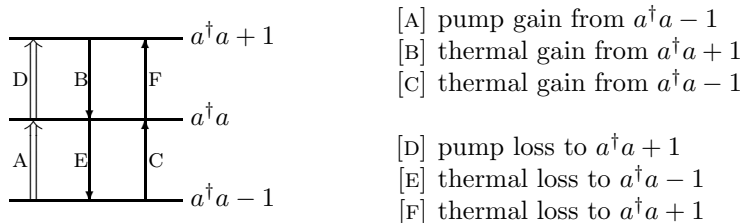


FIG. 7: Probability fluxes representing the gain and loss terms in the OAM master equation for a diagonal photon state. The labeling agrees with the one in Eq. (53).

Another remark concerns the connection between the decay constant A and the quality factor Q of the resonator. Per definition the energy stored decreases to $1/e$ -th of its initial value while the field undergoes Q cycles,

$$e^{-At} = e^{-1} \quad \text{for} \quad \omega t = 2\pi Q : A = \frac{\omega}{2\pi} / Q. \quad (52)$$

In the Garching micromaser experiments one has $\omega \cong 2\pi \times 21.5$ GHz, and quality factors of $Q \cong 10^9 \cdots 10^{10}$ have been achieved, so that the photon life time $1/A$ can be as large as a few hundred microseconds.

One-atom maser: Steady state. General matters

The OAM master equation (31) with (32), (41), and (45) does not contain any terms that are sensitive to the phase of the photon field.⁶ Another way of putting this states that the diagonals of the number-state matrix of ρ are dynamically uncoupled. Therefore, a state ρ which at one time is diagonal in this sense, stays diagonal for all times. A diagonal state is represented by a state operator ρ that depends solely on the product $a^\dagger a$, the photon number operator, but not on the ladder operators a and a^\dagger individually: $\rho = \rho(a^\dagger a)$. The numbers $\rho(n) = \langle n | \rho(a^\dagger a) | n \rangle$ are the probabilities to find n photons in the resonator.

⁶In more technical terms this statement says that (31) is invariant under the unitary transformation $\rho \rightarrow U^\dagger \rho U$ with $U = \exp(i\chi a^\dagger a)$ where χ is an arbitrary (constant) phase angle.

For such a diagonal state, the master equation (31) is particularly transparent. It constitutes a third central result of micromaser theory:

Master equation for diagonal states
of the one-atom maser:

$$\begin{aligned}
\frac{\partial}{\partial t} \rho_t(a^\dagger a) = & \quad r \sin^2 [\varphi(a^\dagger a)^{1/2}] \rho_t(a^\dagger a - 1) \quad \text{[A]} \\
& + A(\nu + 1)(a^\dagger a + 1) \rho_t(a^\dagger a + 1) \quad \text{[B]} \\
& \quad + A\nu a^\dagger a \rho_t(a^\dagger a - 1) \quad \text{[C]} \\
& - r \sin^2 [\varphi(a^\dagger a + 1)^{1/2}] \rho_t(a^\dagger a) \quad \text{[D]} \\
& \quad - A(\nu + 1) a^\dagger a \rho_t(a^\dagger a) \quad \text{[E]} \\
& \quad - A\nu (a^\dagger a + 1) \rho_t(a^\dagger a) \quad \text{[F]}
\end{aligned}
\tag{53}$$

The six terms on the right-hand side possess obvious meanings. These are stated in the probability flux diagram of Fig. 7.

In the steady state $\rho^{(\text{SS})}$ of (53) — which is, of course, also the steady state of (31) — the gains and losses of $\rho(a^\dagger a)$ have to add up to zero. A rearrangement of the right-hand-side terms in (53),

$$\begin{aligned}
& r \sin^2 [\varphi(a^\dagger a)^{1/2}] \rho^{(\text{SS})}(a^\dagger a - 1) \quad \text{[A]} \\
& \quad + A\nu a^\dagger a \rho^{(\text{SS})}(a^\dagger a - 1) \quad \text{[C]} \\
& \quad - A(\nu + 1) a^\dagger a \rho^{(\text{SS})}(a^\dagger a) \quad \text{[E]} \\
& = r \sin^2 [\varphi(a^\dagger a + 1)^{1/2}] \rho^{(\text{SS})}(a^\dagger a) \quad \text{[D]} \\
& \quad + A\nu (a^\dagger a + 1) \rho^{(\text{SS})}(a^\dagger a) \quad \text{[F]} \\
& \quad - A(\nu + 1)(a^\dagger a + 1) \rho^{(\text{SS})}(a^\dagger a + 1), \quad \text{[B]}
\end{aligned}
\tag{54}$$

combines them into two groups of three. Now, observe that the replacement $a^\dagger a \rightarrow a^\dagger a + 1$ turns the [A,C,E] group into the [D,F,B] group. By induction we therefore conclude that the value of the [A,C,E] group is the same for each value of $a^\dagger a$. But for $a^\dagger a = 0$ it is zero. So we arrive at the two-term

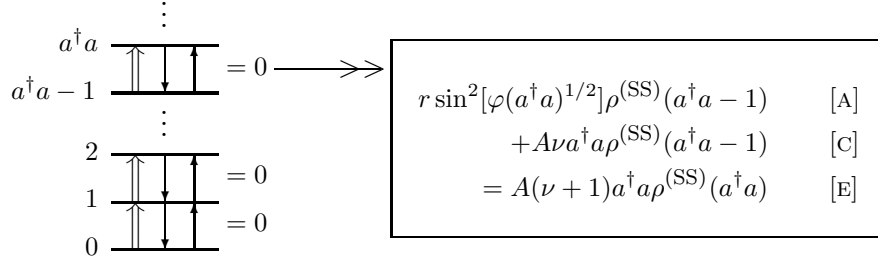


FIG. 8: In steady state the probability fluxes obey a detailed balance between neighboring photon numbers. The terms are labeled the same way as in Eq. (53) and in Fig. 7.

recurrence relation

$$A(\nu + 1)a^\dagger a \rho^{(\text{SS})}(a^\dagger a) = \left(r \sin^2[\varphi(a^\dagger a)^{1/2}] + A\nu a^\dagger a \right) \rho^{(\text{SS})}(a^\dagger a - 1), \quad (55)$$

which is equivalent to the three-term relation (54) but considerably simpler.

The transition from (54) to (55) recognizes the detailed balance in steady state, illustrated in Fig. 8. It comes about because the photon number ladder ends at the $a^\dagger a = 0$ rung.

The recurrence relation (55) can be solved immediately, and we obtain a fourth central result of micromaser theory:

The steady state of the one-atom maser,
pumped by resonant \rightleftharpoons atoms, is given by

$$\rho^{(\text{SS})}(a^\dagger a) = \rho^{(\text{SS})}(0) \prod_{n=1}^{a^\dagger a} \left[\frac{\nu}{\nu + 1} + \frac{r/A}{\nu + 1} \frac{\sin^2(\varphi\sqrt{n})}{n} \right], \quad (56)$$

where the value of $\rho^{(\text{SS})}(0)$ is determined
by the normalization of $\rho^{(\text{SS})}$ to unit trace.

We note that this steady state is determined uniquely by three numbers: the thermal photon number ν , the accumulated Rabi angle φ , and the ratio r/A

of the pump and the decay rates. This ratio tells us how many pump atoms traverse the resonator (on average) during one photon life time. Therefore, we call r/A the effective pump rate.⁷

A simple, but necessary, check of consistency is provided by the consideration of the $r = 0$ case, the case of an unpumped resonator. The steady state of (56) is then the thermal state ρ_{th} of (47), as it must be.

One-atom maser: Steady state. Examples

For fixed values of the effective pump rate r/A and the thermal photon number ν , the steady state of the OAM is traditionally studied as a function of the so-called ‘pump parameter’ $\theta \equiv \varphi\sqrt{r/A}$. Why this scaling of the Rabi angle appears convenient will become plausible later.

For a certain OAM steady state ρ — for simplicity, we drop the superscript of $\rho^{(\text{SS})}$ until we start considering the time dependence of ρ again — the fundamental statistical quantities of interest are mean the photon number $\langle a^\dagger a \rangle = \text{tr}\{a^\dagger a \rho\}$ and its normalized variance,

$$\frac{\langle (a^\dagger a)^2 \rangle - \langle a^\dagger a \rangle^2}{\langle a^\dagger a \rangle}. \quad (57)$$

This quantity (or its square root) is known under various names in the literature,⁸ such as ‘Fano factor,’ or ‘Mandel’s Q parameter,’ or ‘Fano-Mandel measure.’ We prefer the first one in this list. The normalization in (57) is to the value of a Poissonian distribution (as in a coherent state of the harmonic oscillator or a classical state of the radiation field),

$$\rho(n) \Big|_{\text{Poisson}} = \frac{1}{n!} \langle a^\dagger a \rangle^n \exp(-\langle a^\dagger a \rangle), \quad (58)$$

for which $\langle (a^\dagger a)^2 \rangle - \langle a^\dagger a \rangle^2 = \langle a^\dagger a \rangle$. With this normalization comes the jargon of calling a state ρ ‘superpoissonian’ if its Fano factor exceeds unity, and ‘subpoissonian’ if it is less than unity. An example for a superpoissonian state is the thermal state of Eq. (47); its Fano factor equals $\nu + 1$.

⁷In the micromaser literature the symbol N_{ex} is frequently used as an abbreviation for r/A where the subscript ‘ex’ is a reminder of ‘excited.’ We do not adopt this custom.

⁸These names derive from a 1947 paper by Fano [7] and a 1979 paper by Mandel [8], I believe.

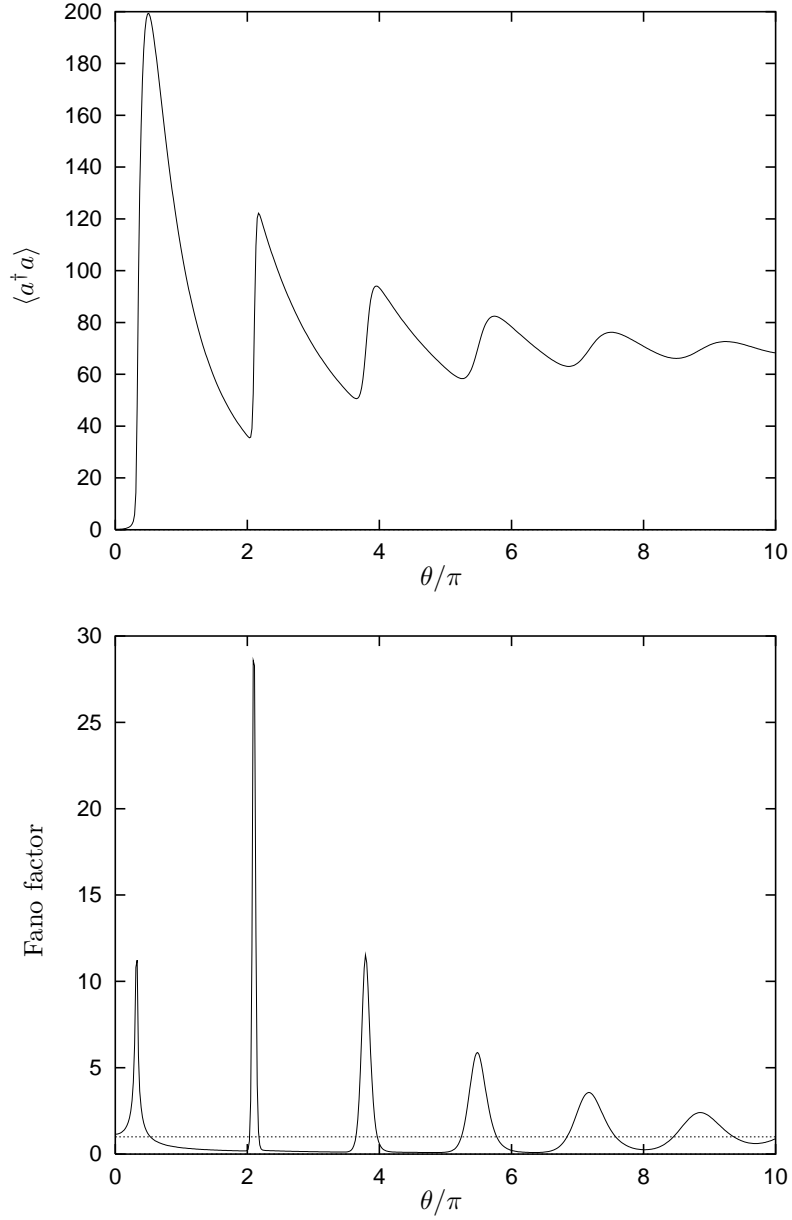


FIG. 9: Mean photon number and Fano factor in the OAM steady state for an effective rate of $r/A = 200$ and a thermal photon number of $\nu = 0.15$, as a function of the pump parameter θ in the range from $\theta = 0$ to $\theta = 10\pi$.

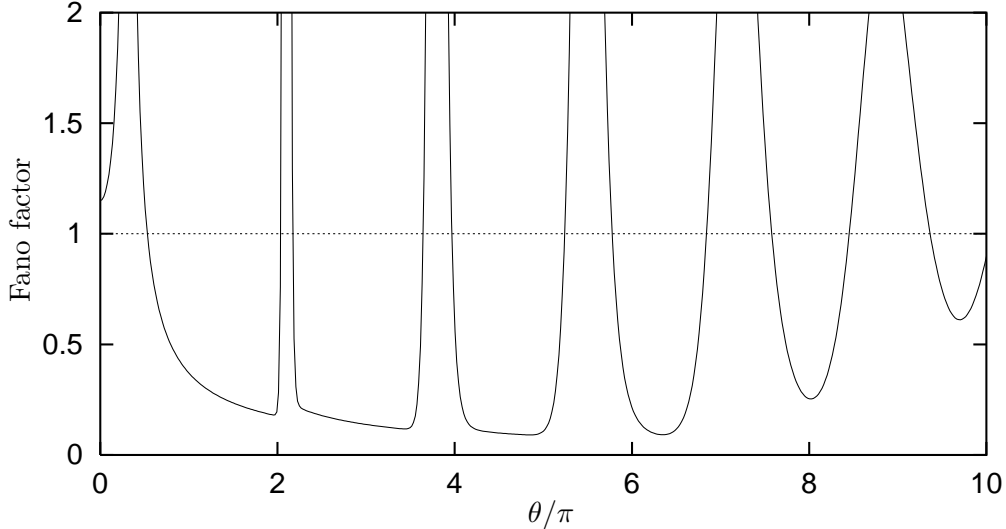


FIG. 10: Fano factor in the OAM steady state for an effective rate of $r/A = 200$ and a thermal photon number of $\nu = 0.15$, as a function of the pump parameter in the range $0 \leq \theta/\pi \leq 10$.

In Fig. 9 the dependence of the photon number and the Fano factor on the pump parameter θ is shown for an effective pump rate of $r/A = 200$ and $\nu = 0.15$ thermal photons. As θ increases from $\theta = 0$, we see an initial rapid growth of both the photon number and the Fano factor. Both numbers reach a maximum and then decrease toward a minimum near $\theta = 2\pi$. This pattern repeats itself roughly with a θ period of 2π .

The maximal value of $\langle a^\dagger a \rangle$, reached near $\theta = \pi/2$, is very close to 200, the value of the effective pump rate. Thus, for this pump parameter the interaction time is just right to ensure that almost all atoms emit a photon into the resonator. At the minimum near $\theta = 2\pi$, by contrast, a large fraction of the atoms do not emit. The interaction time is longer, so that the atoms have a good chance to undergo a complete Rabi cycle $|\uparrow\rangle \rightarrow |\rightarrow\rangle \rightarrow |\downarrow\rangle$ and leave the resonator in the excited state.

The bottom part of the plot of the Fano factor in Fig. 9 is enlarged in Fig. 10. We observe that there are large θ intervals in which the Fano factor is less than one, thus indicating a subpoissonian state of the photon field. It is clear that such states can be realized experimentally, since a very precise

control of the parameters r/A , ν , and θ is not necessary to stay inside the appropriate parameter range.

A look at the histograms in Fig. 11 might be helpful in understanding why the Fano factor covers such a large range of values. For reference each histogram is compared with a corresponding Poissonian one with the same mean number of photons. Whereas we have an almost poissonian distribution for $\theta = \pi/2$ (at the maximum of the $\langle a^\dagger a \rangle$), the distribution for $\theta = 0.32442\pi$ is much broader than the Poissonian one, and that for $\theta = 2\pi$ is much narrower. In these cases it is easily understood that the respective Fano factors are close to, much larger than, or much smaller than unity. A different situation is observed for $\theta = 2.09$ where, according to Fig. 9, the Fano factor is particularly large. In Fig. 11 we recognize the reason for that: there are two narrow peaks — each subpoissonianly narrow — separated by many photon numbers n . As a consequence, the Fano factor, which is a global property of the distribution, is enormous.

The notion of the ‘maser threshold’ is also most easily understood in the context of such histograms. The thermal state (47) is surely below threshold by any definition. Likewise the poissonian state (58), which is so typical for the output of a laser, is certainly above threshold. A striking difference between the two is that the maximum of the poissonian state is at a large photon number n , whereas in the thermal state the largest probability is the one for zero photons. This invites the following criterion based on the relative size of $\rho(0)$, the probability for no photons, and $\rho(1)$, that for one photon:

$$\begin{aligned} \rho(0) > \rho(1) & : \quad \text{below threshold,} \\ \rho(0) = \rho(1) & : \quad \text{at threshold,} \\ \rho(0) < \rho(1) & : \quad \text{above threshold.} \end{aligned} \tag{59}$$

In view of the recurrence relation (55), the explicit OAM version reads

$$\frac{r}{A} \sin^2(\varphi) \begin{cases} < \\ = \\ > \end{cases} 1 : \quad \begin{cases} \text{below} \\ \text{at} \\ \text{above} \end{cases} \text{threshold.} \tag{60}$$

In particular, if the effective rate r/A is large, the threshold value of φ is so small that $\sin^2(\varphi)$ can be replaced by φ^2 , and then we have simply $\theta = 1$ at the maser threshold. This is one reason why the pump parameter θ is

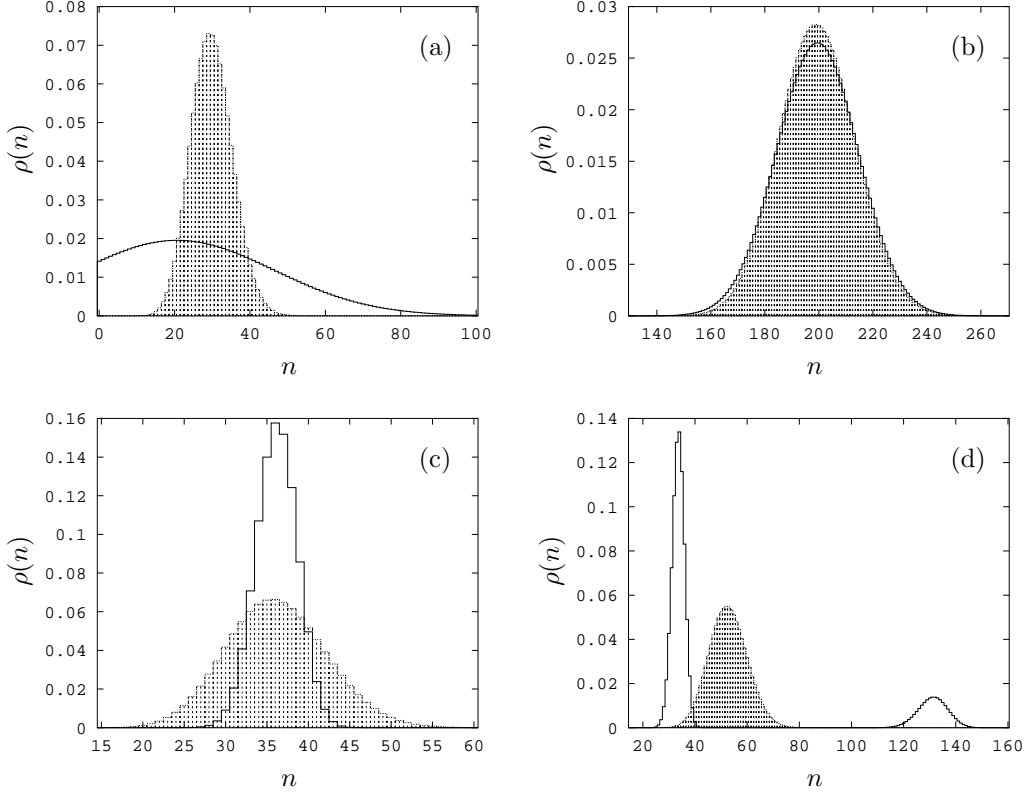


FIG. 11: Histograms for the photon number distribution in the OAM steady state for an effective rate of $r/A = 200$ and a thermal photon number of $\nu = 0.15$. The plots are for (a) $\theta = 0.32442\pi$ (i. e., $\varphi = 4.129^\circ$), (b) $\theta = \pi/2$ (i. e., $\varphi = 6.364^\circ$), (c) $\theta = 2\pi$ (i. e., $\varphi = 25.46^\circ$), and (d) $\theta = 2.09\pi$ (i. e., $\varphi = 26.60^\circ$). The solid line shows the actual distribution. The broken line with the shaded area underneath shows the corresponding Poisson distribution with the same mean photon number. The respective mean photon numbers $\langle a^\dagger a \rangle$ are (a) 30.14, (b) 199.44, (c) 36.25, and (d) 52.72. The Fano factors equal (a) 12.56, (b) 1.153, (c) 0.214, and (d) 28.68.

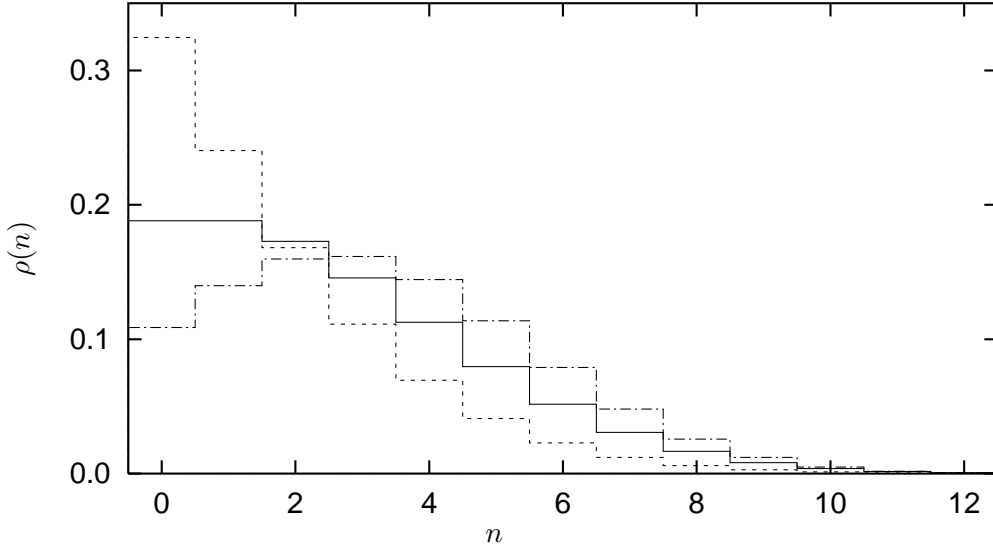


FIG. 12: Histograms for the photon number distribution in the OAM steady state for an effective pump rate of $r/A = 4$ and $\nu = 0.1$ thermal photons. The plot shows the histograms for three different Rabi angle: $\varphi = 30^\circ$ (line —, at threshold), $\varphi = 25^\circ$ (line - - -, below threshold), and $\varphi = 35^\circ$ (line - · - · -, above threshold).

sometimes preferred over the unscaled Rabi angle φ . These matters are illustrated in Fig. 12 where the value $r/A = 4$ is chosen for the effective rate, so that $\varphi = 30^\circ$ holds at the threshold. We note that the thermal photon number ν plays no role in (60).

The threshold concept has its obvious limitations when the photon number distribution may have more than one peak, as realized in the $\theta = 2.09$ case of Fig. 11. More interesting is the question of how many minima and maxima are there and at which n values. The answer is obtained after first recognizing this consequence of the recurrence relation (55):

$$\begin{aligned} \text{if } \frac{r}{A} \sin^2(\varphi\sqrt{n}) > n \text{ then } \rho(n) > \rho(n-1), \\ \text{if } \frac{r}{A} \sin^2(\varphi\sqrt{n}) < n \text{ then } \rho(n) < \rho(n-1). \end{aligned} \quad (61)$$

In this way the n ranges in which $\rho(n)$ decreases or increases monotonically are determined. At the switch-over values we find the maxima and minima

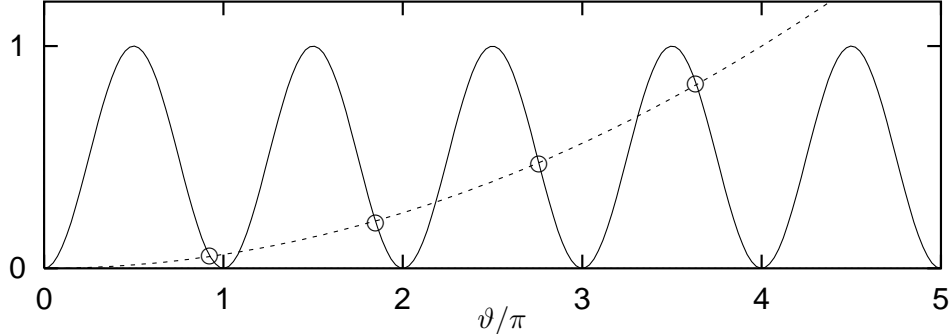


FIG. 13: The two functions of (62) are plotted for $0 \leq \vartheta/\pi \leq 5$. The pump parameter θ has the value of 4π . The intersections marked with a little circle \circ determine the maxima in the photon number distribution, the other intersections determine the minima.

in the photon number distribution. The conditions (61) acquire a more universal appearance when we introduce a new variable $\vartheta \equiv \varphi\sqrt{n}$. Then we have

$$\begin{aligned} \sin^2(\vartheta) &> (\vartheta/\theta)^2 && \text{between minima and maxima,} \\ \sin^2(\vartheta) &< (\vartheta/\theta)^2 && \text{between maxima and minima,} \end{aligned} \quad (62)$$

where the pump parameter $\theta = \varphi\sqrt{r/A}$ appears naturally. This is another reason for using θ rather than φ . In passing we mention that the critical ϑ values, for which $\sin^2(\vartheta) = (\vartheta/\theta)^2$ holds, play a great role in the semiclassical theory of the micromaser. In the context of the quantum treatment discussed here, they determine the n values of the extrema in the photon number distribution. This is illustrated in Fig. 13. The corresponding histogram of $\rho(n)$ should show four maxima, and in Fig. 14 it does indeed. Of course, not all maxima have to be as pronounced as the two in the $\theta = 2.09\pi$ case of Fig. 11 (d). Again we note that, as in (60), the thermal photon number ν is irrelevant in (62). The number of the extrema in the histogram of the photon number distribution as well as their locations are solely determined by the value of θ . Naturally, further details may depend strongly on the value of ν .

In the discussion of the plots in Fig. 9 we had remarked that the pattern roughly repeats itself with a θ period of 2π . That may be true for the parameter range of Fig. 9, but for other values of the effective rate r/A , other

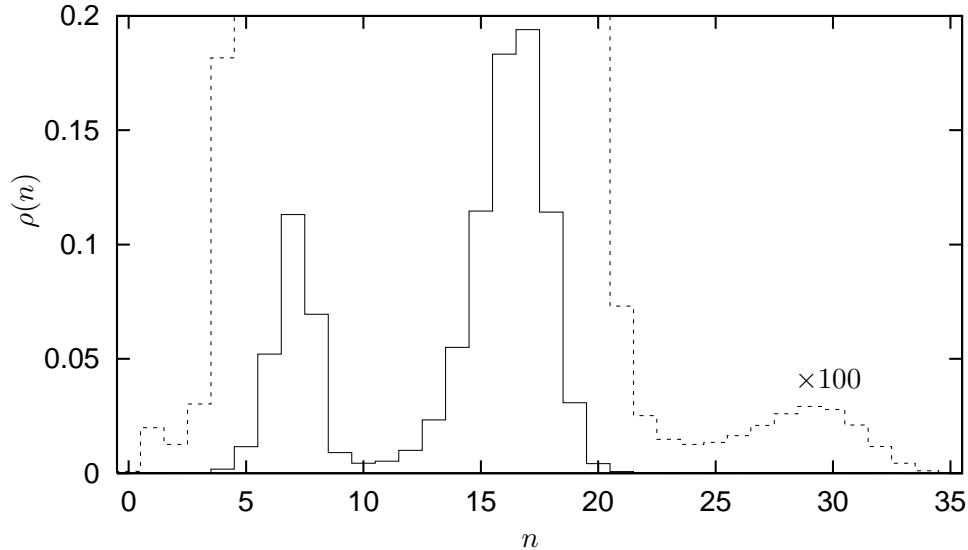


FIG. 14: Histogram for a steady state with $\theta = 4\pi$ (actually: $r/A = 36$, $\nu = 0.15$, $\varphi = 2\pi/3$). The dashed line shows $100\rho(n)$. Consistent with Fig. 13, we note four maxima: $\rho(1) = 0.00020$, $\rho(7) = 0.11316$, $\rho(17) = 0.19397$, and $\rho(29) = 0.00029$.

thermal photon numbers ν , or other θ ranges matters tend to be different. As an example we take a look at Fig. 15 where the rate is much smaller, namely $r/A = 6$, and the temperature much higher, $\nu = 2$. Rather than the regular pattern of Fig. 9 we observe an irregular behavior. The initial oscillation is quickly damped away, but builds up again at larger values of the Rabi angle φ , that is: at longer interaction times. This phenomenon is reminiscent of and related to the so-called Jaynes-Cummings revivals. Strictly speaking, the latter occur when a two-level atom is in permanent (resonant) interaction with photons of one field mode. The Rabi angle is then proportional to the elapsed interaction time. Although the OAM plots in Fig. 15 refer to many atoms with a fixed common interaction time, it is nevertheless clear that the revivals in this figure are similar — both in their appearance and in their physical origin — to those Jaynes-Cummings revivals.

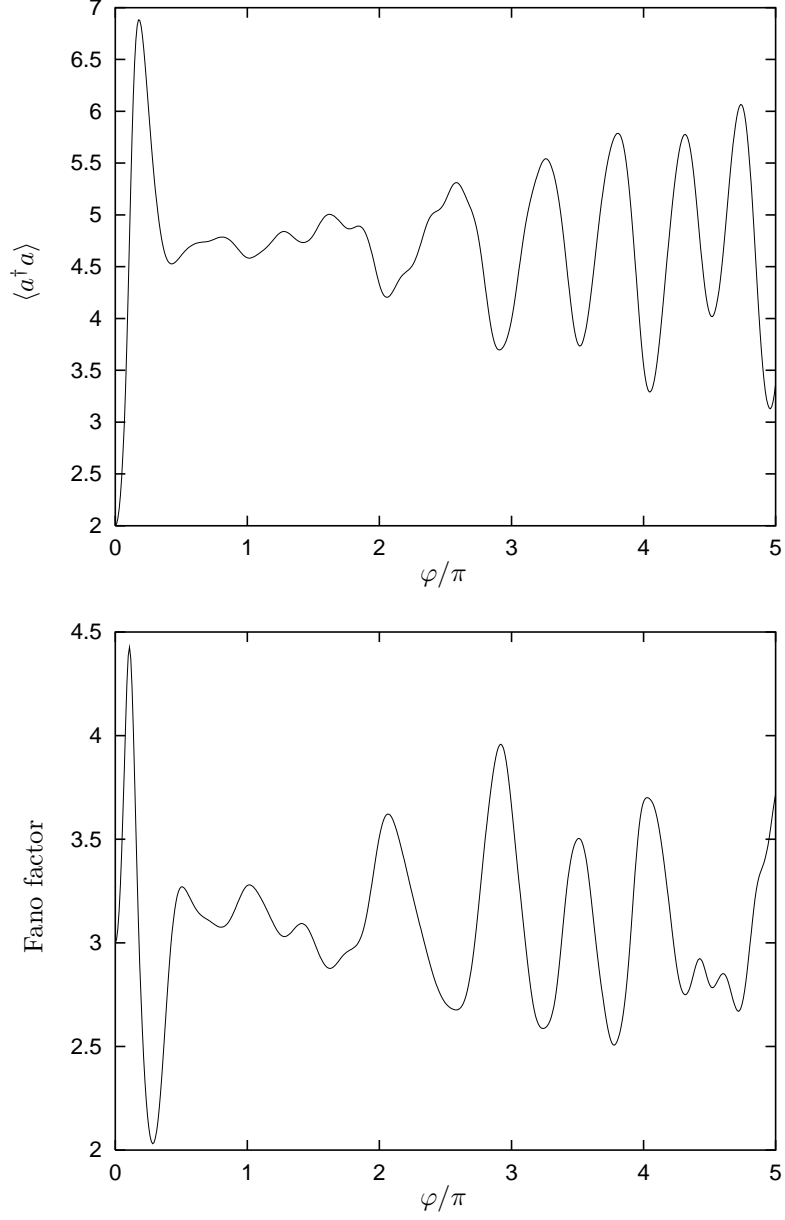


FIG. 15: Mean photon number and Fano factor in the OAM steady state for an effective rate of $r/A = 6$ and a thermal photon number of $\nu = 2$, as a function of the Rabi angle φ in the range from $\varphi = 0$ to $\varphi = 5\pi$.

One-atom maser: Steady state. Energy balance

One cannot measure the photon state itself in micromaser experiments — by counting photons, say — because that would violate the requirement of a very large quality factor of the resonator. The experimenter can only look at the atoms emerging from the resonator after having interacted with the photon field. The experimental data consists of the statistics of the final atomic states. For instance, one could count which fraction ends up in the excited \rightleftharpoons state and which fraction emits a photon and comes out in the deexcited \leftleftharpoons state. It is an essential task of OAM theory to compute these fractions, and many other statistical properties of the emerging atoms, and to relate them, whenever possible, to the properties of the photon state inside the resonator.

The calculation of the probability for a $\rightleftharpoons \rightarrow \leftleftharpoons$ transition during the passage of the atom through the resonator is based on the result (25). We recall that $|\rightleftharpoons, n\rangle \rightarrow |\leftleftharpoons, n+1\rangle$ happens with probability $\sin^2(\varphi\sqrt{n+1})$. Therefore, if the atom encounters a state

$$\rho(a^\dagger a) = \sum_{n=0}^{\infty} |n\rangle \rho(n) \langle n|, \quad (63)$$

then the total transition probability is given by

$$\begin{aligned} \text{prob}(\rightleftharpoons \rightarrow \leftleftharpoons) &= \sum_{n=0}^{\infty} \rho(n) \sin^2(\varphi\sqrt{n+1}) \\ &= \text{tr}\{\rho \sin^2[\varphi(aa^\dagger)^{1/2}]\} \\ &= \langle \sin^2[\varphi(aa^\dagger)^{1/2}] \rangle. \end{aligned} \quad (64)$$

This probability can be computed immediately once the steady state ρ has been determined in accordance with (56). In a series of challenging experiments, actual measurements have been performed (see [1] and the references therein, in particular [9] and [10]), and very good agreement with the theoretical predictions has been found.

When we multiply the transition probability (64) by the beam rate r and the energy per photon $\hbar\omega$, we obtain the rate at which the photon field gains energy: $r \hbar\omega \text{prob}(\rightleftharpoons \rightarrow \leftleftharpoons)$. In view of Eq. (50), the energy loss rate is likewise given by the product of the decay rate A , the energy per photon $\hbar\omega$, and the difference between the actual mean photon number $\langle a^\dagger a \rangle$ and

the thermal photon number ν : $A\hbar\omega(\langle a^\dagger a \rangle - \nu)$. In steady state these two rates must be equal. After canceling the common factor of $\hbar\omega$ we thus arrive at a fifth central result of micromaser theory:

In the steady state of a one-atom maser, pumped by resonant \rightleftharpoons atoms, the energy balance implies the equality

$$\underbrace{r\langle \sin^2[\varphi(aa^\dagger)^{1/2}] \rangle}_{\propto \text{energy gain rate}} = \underbrace{A(\langle a^\dagger a \rangle - \nu)}_{\propto \text{energy loss rate}}. \quad (65)$$

The expectation value on the left-hand side can be measured experimentally.

We emphasize that by determining the fraction of atoms that have emitted a photon one can experimentally measure the mean photon number inside the resonator. The link between the two quantities is provided by the theory of the OAM and stated in (65).

The way in which we derived this statement simply appealed to the physical significance of the expressions on the two sides. A more formal derivation employs the two-term recurrence relation (55) in the form

$$r \sin^2[\varphi(aa^\dagger)^{1/2}] \rho(a^\dagger a) = A[(\nu + 1)\rho(a^\dagger a + 1) - \nu\rho(a^\dagger a)](a^\dagger a + 1). \quad (66)$$

Upon taking the trace on both sides, we find

$$r\langle \sin^2[\varphi(aa^\dagger)^{1/2}] \rangle = A(\nu + 1)\langle a^\dagger a \rangle - A\nu\langle a^\dagger a + 1 \rangle, \quad (67)$$

which, after an elementary simplification, is recognized to be identical to the statement in (65).

One-atom maser: Trapped states

At zero temperature there are no thermal photons: $\nu = 0$. Then the contributions [C] and [E] are not present in Eqs. (53) and (54) and in Figs. 7 and 8.

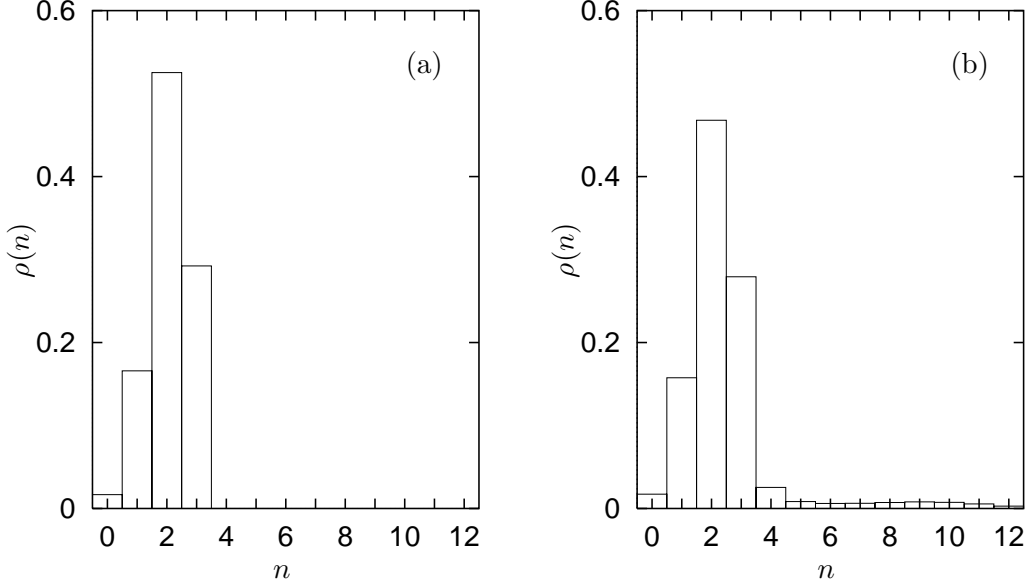


FIG. 16: Histograms for the OAM steady states obtained for $r/A = 10$, $\varphi = \pi/2$, and (a) $\nu = 0$, (b) $\nu = 0.1$. In case (a) the trapping limits the possible photon numbers to the values $n = 0, 1, 2, 3$. No trapping occurs in case (b).

As a consequence, the steady state (56) of the one-atom maser is particularly simple, viz.

$$\left[\rho^{(\text{SS})}(a^\dagger a) \right] = \rho(a^\dagger a) = \rho(0) \frac{(r/A)^{a^\dagger a}}{(a^\dagger a)!} \prod_{n=1}^{a^\dagger a} \sin^2(\varphi\sqrt{n}). \quad (68)$$

In contrast to the general $\nu \neq 0$ case of (56), here the individual factors of the product might vanish. Thus we note this property of (68):

$$\begin{aligned} &\text{if } \sin^2(\varphi\sqrt{N}) = 0 \text{ holds for } N = 1, 2, 3, \dots, \\ &\text{then } \rho(a^\dagger a) = 0 \text{ holds for } a^\dagger a \geq N. \end{aligned} \quad (69)$$

One says that the photon number is ‘trapped’ below $a^\dagger a = N$.

Such trapped states are very characteristic of the OAM dynamics. For purely energetic reasons, the mean photon number $\langle a^\dagger a \rangle$ could be as large

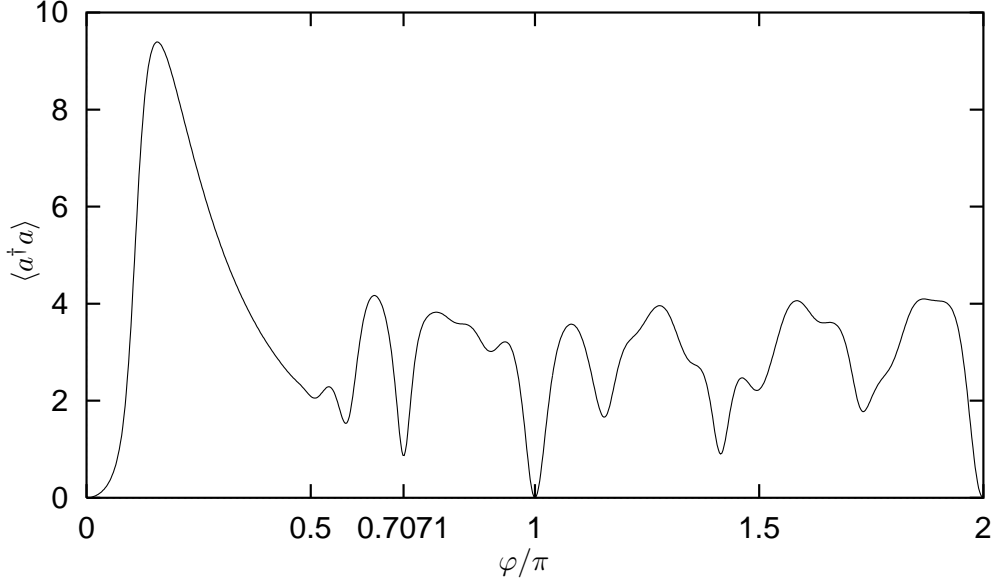


FIG. 17: Mean photon number in the OAM steady states obtained for an effective pump rate of $r/A = 10$ at zero temperature ($\nu = 0$), as a function of the Rabi angle φ in the range $0 \leq \varphi \leq 2\pi$. Please note the dips at $\varphi = \pi$ and $\varphi = 2\pi$ that indicate trapped vacuum states.

as the effective pump rate r/A [recall Eq. (65), here for $\nu = 0$]. The specific OAM dynamics, however, may limit the photon number to much smaller values. We illustrate this in Fig. 16, where the histogram for $\varphi = \pi/2$, that is: $N = 4$ in (69), shows nonzero probabilities only for the photon numbers $n = 0, 1, 2, 3$, although the effective rate, $r/A = 10$, is more than twice as large. A second plot in this figure demonstrates how a small number of thermal photons ($\nu = 0.1$) removes the trapping.

A very remarkable trapped state is the trapped vacuum state, which is realized if φ equals an integer multiple of π . In Fig. 17, the trapped vacuum states at $\varphi = \pi$ and $\varphi = 2\pi$ are visible as pronounced dips in the plot of the mean photon number. Note also the minimum at $\varphi = \pi/\sqrt{2}$ that corresponds to a trapping below $a^\dagger a = 2$.

When the vacuum is trapped, the atoms perform one or more complete Rabi cycles while traversing the resonator. In other words, each atom first emits a photon and then reabsorbs it — perhaps repeatedly — eventually

leaving the resonator in the excited state \pm in which it entered. This is, of course, the $n = 0$ situation of Eq. (27). Under these circumstances it does not matter how frequent the one-atom events are, nor if they occur in accordance with the Poisson statistics of (28). It is simply impossible to get photons into the resonator.

Approximations in one-atom-maser theory

A direct experimental demonstration of the trapped vacuum state has not been achieved as yet. To understand why, we recall that the theoretical result (68) is based upon various approximations. Let us reconsider them and their significance for the trapped vacuum state. In this context, the most important approximations are:

The interaction time is assumed to be the same for all atoms.

This assumption has two aspects:

The atoms should have the same velocity v .

Differing velocities lead to differing Rabi angle φ . Fortunately, however, the trapping condition requires $\varphi = \pi$, where $\sin^2(\varphi)$ has a minimum. Therefore, deviations from the ideal φ value of π do not change anything to first order. A velocity control to about one percent is good enough, and that can be realized experimentally.

Atomic decays to other levels do not occur.

The Rydberg states of Fig. 2 do not meet this condition sufficiently well; a few percent of the atoms make ultraviolet transitions to low lying levels and thus stop interacting with the photons in the privileged mode before they actually leave the resonator. Therefore, one has to use Rydberg states that live even longer, the so-called circular states in which both the angular and the magnetic quantum number are maximal [11]. The masing of such circular states has already been demonstrated experimentally [12]. A one-atom-maser operation is likely to be realized in the near future.

The transition frequency Ω of Eq. (6) is assumed to be equal to the photon frequency ω for all atoms.

This has also two main aspects:

The resonator must be mechanically stable.

Apparently one does not have to worry much about this. I am told that the detuning resulting from mechanical instabilities is less than 100 Hz.⁹

Electric stray fields must be small.

Here the concern is about Stark shifts of the atomic levels. Inasmuch as the stray fields are prominent only in the entry and exit ports of the resonator, and not so much inside where the relevant atom-photon interaction takes place, they are not very critical. In other experiments, however, in which the atoms are prepared in coherent superpositions of \rightleftharpoons and \leftrightharpoons , stray fields are a great nuisance because the differential Stark shift changes the phase relations between \rightleftharpoons and \leftrightharpoons and thus may destroy the desired superposition.

The photon damping is neglected during the atom-photon interaction.

This is harmless. Indeed, the Jaynes-Cummings model can be extended by the inclusion of photon damping. One then finds [13] that the trapping condition of (69) is altered slightly, but trapping still exists.

Collective events are not taken into account.

This is a critical point. We shall deal with it in some detail.

Two-atom events

A typical number for AL/v in the Garching micromaser experiments is $10^{-4}\pi$. For an effective beam rate of $r/A = 10$, the probability (30) for a one-atom event is then $\exp(-2rL/v) = \exp[-2(r/A) \times (AL/v)] = 99.4\%$. In this situation, only 0.6% of the atoms participate in collective events, and most of those in two-atom events.

Although these collective events are very rare, they may cause dramatic effects nevertheless. In particular, they destroy the trapped vacuum state completely. The physical reason is the following. After two atoms, say, have been in the resonator simultaneously, the photon field is no longer in the vacuum state, there are nonzero probabilities for one or two photons. Single atoms that follow will then emit more photons and so drive the maser field

⁹A detuning should not be compared with the transition frequency of ~ 21.5 GHz, but rather with the Rabi frequency of ~ 14 kHz.

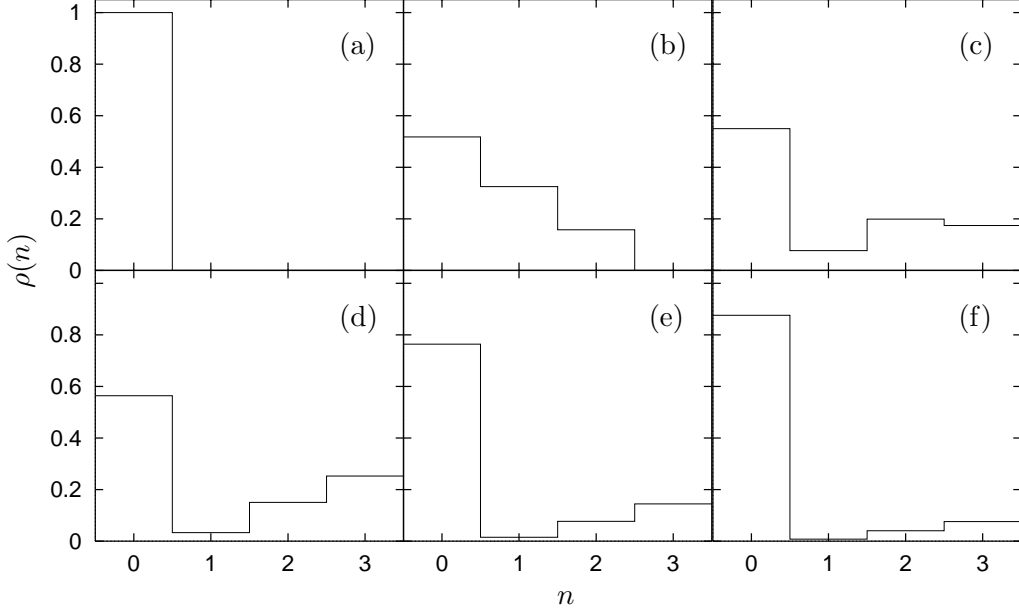


FIG. 18: Histograms of (a) the trapped vacuum state; (b) the state immediately after the passage of an atom pair; and after subsequent one-atom operation for a period during which (c) two, (d) five, (e) one hundred, or (f) two hundred one-atom events occur on average.

further away from the vacuum. This is demonstrated in Fig. 18. Eventually, after a large number of one-atom events, the maser field will return to the vacuum state. The analysis given below shows that *very many* one-atom events are needed to undo the damage caused by a single two-atom event, so many indeed that another two-atom event is very likely to occur in the meantime. Therefore, we have to conclude that, despite their rare occurrence, the collective events prevent the observation of the trapped vacuum state in a micromaser with a poissonian pump beam.

Consider the OAM dynamics of Eq. (53) at zero temperature ($\nu = 0$) and for $\varphi = \pi$,

$$\begin{aligned} \frac{\partial}{\partial t} \rho_t(a^\dagger a) = & r_1 \sin^2 \left[\pi (a^\dagger a)^{1/2} \right] \rho_t(a^\dagger a - 1) + A (a^\dagger a + 1) \rho_t(a^\dagger a + 1) \\ & - \left\{ r_1 \sin^2 \left[\pi (a^\dagger a + 1)^{1/2} \right] + A a^\dagger a \right\} \rho_t(a^\dagger a), \end{aligned} \quad (70)$$

where r_1 is the rate of one-atom events; its relation to the beam rate r is given by $r_1 = r \exp(-2rL/v)$. One verifies easily that the vacuum state $\rho_{\text{vac}} = \delta(a^\dagger a, 0)$ is the steady state of (70).

For $\varphi = \pi$, the trapping condition is not only obeyed by $N = 1$, but also by $N = 4, 9, 16, \dots$, so that the threshold from three to four photons cannot be crossed by one-atom events. Now, after a two-atom event has happened to an initial vacuum state, the probabilities for one or two photons will be nonzero, but those for three or more photons still vanish. As long as only one-atom events occur thereafter, the probabilities for more than three photons remain zero. Thus a fitting ansatz for $\rho_t(a^\dagger a)$ is

$$\rho_t = \alpha_t^{(0)} \delta(a^\dagger a, 0) + \alpha_t^{(1)} \delta(a^\dagger a, 1) + \alpha_t^{(2)} \delta(a^\dagger a, 2) + \alpha_t^{(3)} \delta(a^\dagger a, 3), \quad (71)$$

wherein the time-dependent numerical coefficients $\alpha_t^{(0,1,2,3)}$ are the respective probabilities to have no, one, two, or three photons in the resonator. The sum of these probabilities is 100% — this is the normalization of ρ to unit trace — and that requires $\alpha^{(0)} = 1 - \alpha^{(1)} - \alpha^{(2)} - \alpha^{(3)}$.

At $t = 0$, we have $\alpha_0^{(3)} = 0$, of course, and typical numbers for the initial values of $\alpha_t^{(1)}$ and $\alpha_t^{(2)}$ are [14]

$$\alpha_0^{(1)} = \frac{1}{3} [\sin(\pi\sqrt{6})]^2 = 0.3250, \quad \alpha_0^{(2)} = \frac{8}{9} [\sin(\pi\sqrt{3/2})]^4 = 0.1575. \quad (72)$$

As implied by (70), the time dependence of these coefficients is determined by

$$\left[\frac{1}{A} \frac{d}{dt} + \begin{pmatrix} 1 + \frac{r_1}{A} \sin^2(\pi\sqrt{2}) & -2 & 0 \\ -\frac{r_1}{A} \sin^2(\pi\sqrt{2}) & 2 + \frac{r_1}{A} \sin^2(\pi\sqrt{3}) & -3 \\ 0 & -\frac{r_1}{A} \sin^2(\pi\sqrt{3}) & 3 \end{pmatrix} \right] \begin{pmatrix} \alpha_t^{(1)} \\ \alpha_t^{(2)} \\ \alpha_t^{(3)} \end{pmatrix} = 0. \quad (73)$$

The time scale for the return to the vacuum is set by the eigenvalues of this 3×3 matrix, more precisely: by the smallest one. For $r/A = 10$, $r_1/A = 9.937$ these eigenvalues are

$$13.974, \quad 6.7225, \quad 0.063869 = \frac{r_1/A}{155.6}. \quad (74)$$

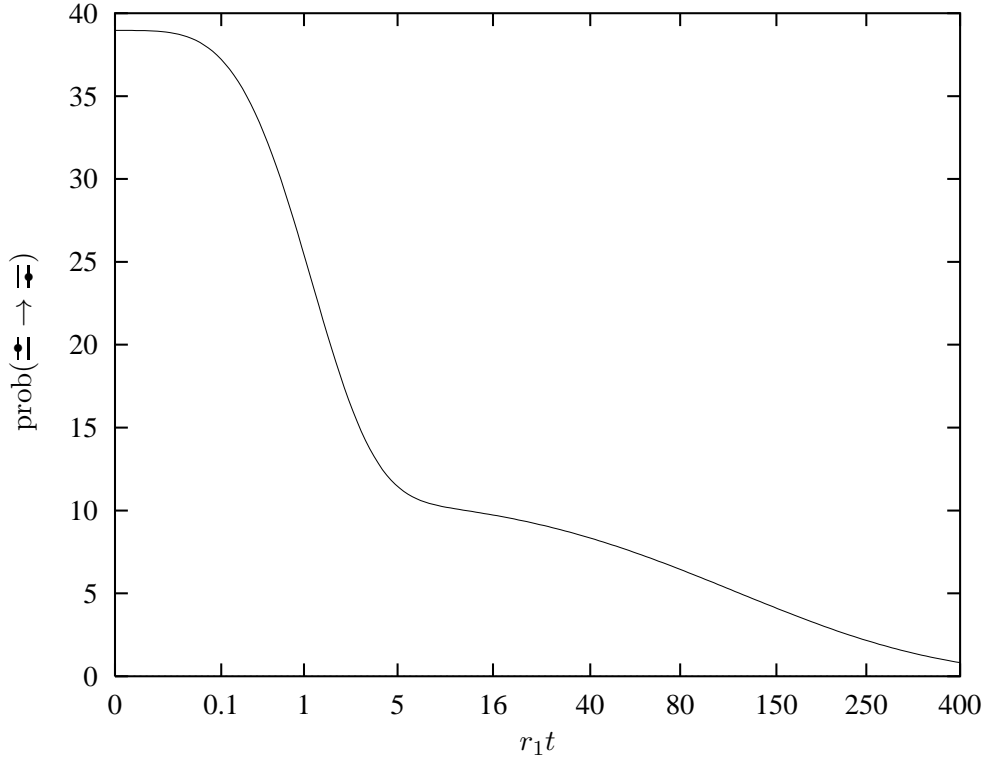


FIG. 19: Time dependence of the emission probability of atoms in one-atom events after the passage of an atom pairs, for $0 \leq t \leq 400/r_1$. The abscissa is linear in $(r_1 t)^{1/4}$.

Please note that the smallest one is *very small* indeed. It takes hundreds of one-atom events to get close to the vacuum state; see Fig. 18 again, where the photon states are reported for $r_1 t = 0, 2, 5, 100, 200$. During such a long time, another collective event is very likely to occur, so that the vacuum state will not be reached at all.

To be more specific, we note that the experimental signature for the trapped vacuum state is the observation of all atoms emerging in the excited $\uparrow\downarrow$ state. Therefore, an appropriate numerical criterion should involve the probability that the atom emits a photon if it traverses the resonator at time t . This probability is given in Eq. (64). For states of the form (71) it

reads

$$\text{prob}_t(\underline{\pm} \rightarrow \overline{\pm}) = \alpha_t^{(1)} \sin^2(\pi\sqrt{2}) + \alpha_t^{(2)} \sin^2(\pi\sqrt{3}). \quad (75)$$

This probability is plotted in Fig. 19. If we now require that 99% of the atoms emerge in the upper state $\underline{\pm}$, then the emission probability must get as small as 1% before we would say that the vacuum state has been reached again. The time $t = 370/r_1$ has to go by for the parameters we have been using consistently, and the probability that at least one more collective event takes place in the meantime is 68.8% [14]. This number is discouragingly large — it is clear that one needs to operate the micromaser with a pump beam that has considerably fewer collective events, if the trapped vacuum state is to be observed.

The small eigenvalue of the 3×3 matrix in (73) is one theoretical indication that very long time scales are present in the dynamics of the micromaser. In this context, it is worth mentioning that very recent experiments [15] have demonstrated the presence of extremely large time scales in rather different dynamical regimes of the micromaser as well.

Correlations among emerging atoms

We have remarked above that the photon state cannot be observed directly in micromaser experiments. The only reproducible data concerns the emerging atoms, more specifically: their statistical properties. Experimental tests of the micromaser theory must therefore compare the measured atom statistics to the theoretically predicted ones. We have seen one elementary example already, in the context of Eq. (65). On the one hand, one can calculate the transition probability (64); on the other hand, it can be measured by counting the atoms that end up in the $\underline{\pm}$ or the $\overline{\pm}$ state.

More subtle are statistical predictions about correlations among emerging atoms. The general theory for their calculation is rather involved [16] and well beyond the scope of this tutorial review. We shall therefore be content with presenting two rather simple examples. They serve the purpose of conveying the spirit in which such calculations are done without requiring too much technical detail.

Consider a OAM at zero temperature ($\nu = 0$) operated with a Rabi angle

of $\varphi = \pi/\sqrt{2}$, so that the trapped state with one photon at most,

$$\rho^{(\text{SS})} = \frac{1}{A + r \sin^2(\pi/\sqrt{2})} \left[A\delta(a^\dagger a, 0) + r \sin^2(\pi/\sqrt{2})\delta(a^\dagger a, 1) \right], \quad (76)$$

is the steady state. The meaning of this $\rho^{(\text{SS})}$ is this: it is to be used for statistical predictions, if nothing else is known. For instance, the (a priori) probability for an atom to end up in the $\overleftarrow{\rightleftharpoons}$ state is

$$\text{tr} \left\{ \sin^2[\pi(a^\dagger a/2)^{1/2}] \rho^{(\text{SS})}(a^\dagger a) \right\} = \frac{A \sin^2(\pi/\sqrt{2})}{A + r \sin^2(\pi/\sqrt{2})}, \quad (77)$$

as stated in Eq. (64).

Now suppose that we have just registered, at $t = 0$, an atom in the $\overleftarrow{\rightleftharpoons}$ state. What is then the probability that the next atom emerges also in the $\overleftarrow{\rightleftharpoons}$ state? We are here asking for a conditional probability, rather than for an a priori probability. The steady state $\rho^{(\text{SS})}$ is not appropriate any more. In its stead we must employ that time dependent state ρ_t which correctly accounts for the imposed conditions. Then

$$\text{prob}_t(\overleftarrow{\rightleftharpoons} \rightarrow \overleftarrow{\rightleftharpoons}) = \text{tr} \left\{ \sin^2[\pi(a^\dagger a/2)^{1/2}] \rho_t \right\} \quad (78)$$

is the transition probability if the next atom comes after the elapse of time t . And the probability that the next atom arrives between t and $t + dt$ is $dt r \exp(-rt)$, where we remind ourselves of the Poisson formula (28). Upon putting things together, we find that the asked-for probability that the next atom also emits a photon is given by

$$\text{prob}(\text{next in } \overleftarrow{\rightleftharpoons}) = \int_0^\infty dt r e^{-rt} \text{tr} \left\{ \sin^2[\pi(a^\dagger a/2)^{1/2}] \rho_t \right\}. \quad (79)$$

We still have to say how the correct ρ_t is calculated. This requires to find (i) the appropriate initial state ρ_0 and (ii) the appropriate master equation for ρ_t .

At $t = 0$, we know that an atom has just been registered in the $\overleftarrow{\rightleftharpoons}$ state. Prior to its passage through the resonator we had no additional information, so that then $\rho^{(\text{SS})}$ applies. Immediately after the observation of the initial $\overleftarrow{\rightleftharpoons}$ atom, however, the photon state is reduced to account for this information,

$$\text{state reduction: } \rho^{(\text{SS})} \longrightarrow \delta(a^\dagger a, 1) \equiv \rho_0. \quad (80)$$

In other words: after the registration of the atom emerging in the $\overleftarrow{\leftarrow}$ state we know with certainty that there is one photon in the resonator.

Until the next atom arrives, there are no other atoms traversing the resonator. Consequently, ρ_t is determined by the master equation (46) of the unpumped resonator (here for $\nu = 0$). So we find first

$$\rho_t = (1 - e^{-At}) \delta(a^\dagger a, 0) + e^{-At} \delta(a^\dagger a, 1), \quad (81)$$

then

$$\text{prob}_t(\overleftarrow{\leftarrow} \rightarrow \overleftarrow{\leftarrow}) = (1 - e^{-At}) \sin^2(\pi/\sqrt{2}), \quad (82)$$

and finally

$$\text{prob}(\text{next in } \overleftarrow{\leftarrow}) = \left(1 - \frac{r}{A}\right) \sin^2(\pi/\sqrt{2}). \quad (83)$$

This answers the question asked above. Compared with the a priori transition probability in (77), this conditional transition probability is smaller.

The time dependent transition probability (82) vanishes for $t = 0$ and approaches $\sin^2(\pi/\sqrt{2})$ for $t \rightarrow \infty$. Both properties are easily understood on physical grounds. At $t = 0$, that is: immediately after the first atom was found in the $\overleftarrow{\leftarrow}$ state, the trapping condition forbids the emission of another photon into the resonator. And if no atom has traversed the resonator for a time long compared to the photon life time $1/A$ — this is the physical significance of the mathematical $t \rightarrow \infty$ limit — the photon field is in the vacuum state, and then the transition probability is given by (25) with $n = 0$ and $\varphi = \pi/\sqrt{2}$.

As another example, we consider again that at $t = 0$ an atom is found in the $\overleftarrow{\leftarrow}$ state, but let us now ask this question: If another atom comes between t and $t + dt$, with which probability will it be in the $\overleftarrow{\leftarrow}$ state as well? Note the difference. Above we were interested in *the next* atom, now in *another* atom. Clearly, the initial state is obtained by the same reduction, viz. that of (80), but now ρ_t is determined by the OAM master equation (70) with $\varphi = \pi/\sqrt{2}$. Rather than (82), we get here

$$\text{prob}_t(\overleftarrow{\leftarrow} \rightarrow \overleftarrow{\leftarrow}) = \underbrace{\frac{A \sin^2(\pi/\sqrt{2})}{A + r \sin^2(\pi/\sqrt{2})}}_{\text{a priori probability}} \underbrace{\left(1 - \exp\left[-\left(A + r \sin^2(\pi/\sqrt{2})\right)t\right]\right)}_{\text{correlation function for } \overleftarrow{\leftarrow} \text{ atoms}}. \quad (84)$$

We recognize that the first factor is the a priori probability of (77), and the second factor is the so-called correlation function. It is a numerical measure for the strength of the correlations among atoms emerging in the \rightleftharpoons state. If the temporal separation is too large — physically: $t \gg 1/A, 1/r$ — there must not be any correlations. Indeed, the correlation function approaches unity for $t \rightarrow \infty$, and the conditional probability (84) equals the a priori probability in this limit, as it should.

These two examples must suffice as illustrations for the typical reasonings that are necessary for the computation of statistical properties of the emerging atoms. Let us just mention that the experimental data refers actually to the statistics of the detector clicks, rather than to the atoms themselves, and therefore the efficiencies of the detectors have to be taken into account as well. Naturally, that introduces further complications which are, however, under good theoretical control.

Acknowledgments

I would like to express my sincere gratitude towards the organizers and the sponsors of the 19th Nathiagali Summer College for the very kind hospitality I experienced in Pakistan and particularly in Nathiagali. I thank especially M. S. Zubairy, K. A. Shoaib, and S. M. Farooqi for treating me so well. The splendid company of I. Ashraf and S. Qamar is unforgettable.

References

- [1] G. Raithel, C. Wagner, H. Walther, L. M. Narducci, and M. O. Scully, *The Micromaser: A proving ground for quantum physics*, in: Ref. [3], pp. 57–121.
- [2] S. Haroche and J. M. Raimond, *Manipulation of nonclassical field states in a cavity by atom interferometry*, in: Ref. [3], pp. 123–170.
- [3] P. R. Berman (ed.), *Cavity Quantum Electrodynamics* (Academic Press, San Diego 1994).
- [4] See, for example,
 - (a) P. Meystre and M. Sargent III, *Elements of Quantum Optics* (Springer-Verlag, Berlin 1990); or

- (b) W. Vogel and D.-G. Welsch, *Lectures on Quantum Optics* (Akademie Verlag, Berlin 1994).
- [5] E. T. Jaynes and F. W. Cummings, Proc. IEEE **51**, 89 (1963).
- [6] (a) S. Haroche, M. Brune, and J. M. Raimond, Europhys. Lett. **14**, 19 (1991);
- (b) B.-G. Englert, J. Schwinger, A. O. Barut, and M. O. Scully, Europhys. Lett. **14**, 25 (1991);
- (c) M. Battocletti, and B.-G. Englert, J. Phys. II (Paris) (in print, November 1994).
- [7] U. Fano, Phys. Rev. **72**, 26 (1947).
- [8] L. Mandel, Opt. Lett. **4**, 205 (1979).
- [9] G. Rempe, H. Walther, and N. Klein, Phys. Rev. Lett. **58**, 353 (1987).
- [10] G. Rempe and H. Walther, Phys. Rev. A **42**, 1650 (1990).
- [11] (a) R. J. Brecha, G. Raithel, C. Wagner, and H. Walther, Opt. Commun. **102**, 257 (1993);
- (b) P. Nussenzveig, F. Bernadot, M. Brune, J. Hare, J. M. Raimond, S. Haroche, and W. Gawlik, Phys. Rev. A **48**, 3991 (1993).
- [12] O. Benson, A. Dost, V. Doebner, G. Raithel, C. Wagner, and H. Walther, to be published.
- [13] (a) H.-J. Briegel and B.-G. Englert, Phys. Rev. A **47**, 3311 (1993);
- (b) H.-J. Briegel, B.-G. Englert, C. Ginzler, and A. Schenzle, Phys. Rev. A **49**, 5019 (1994).
- [14] E. Wehner, R. Seno, N. Sterpi, B.-G. Englert, and H. Walther, Opt. Commun. **110**, 655 (1994).
- [15] O. Benson, G. Raithel, and H. Walther, Phys. Rev. Lett. **72**, 3506 (1994).
- [16] (a) H.-J. Briegel, B.-G. Englert, N. Sterpi, and H. Walther, Phys. Rev. A **49**, 2962 (1994);
- (b) C. Wagner, A. Schenzle, and H. Walther, Opt. Commun. **107**, 318 (1994);
- (c) U. Herzog, Phys. Rev. A **50**, 783 (1994).

Contents

Experimental setup and other introductory remarks	2
Atom-photon interaction (Jaynes-Cummings model)	3
One-atom operation	10
One-atom maser: Dynamics	12
One-atom maser: Steady state. General matters	18
One-atom maser: Steady state. Examples	21
One-atom maser: Steady state. Energy balance	28
One-atom maser: Trapped states	31
Approximations in one-atom-maser theory	34
Two-atom events	35
Correlations among emerging atoms	39
Acknowledgments	42

List of Figures

1	Experimental setup	2
2	Relevant Rb levels	4
3	Before/after	5
4	Rabi frequency as a function of time	6
5	One-atom event	11
6	OAM gain	13
7	Gain and loss	18
8	Detailed balance	20
9	Steady state for $r/A = 200, \nu = 0.15$	22
10	Steady state for $r/A = 200, \nu = 0.15$	23
11	Histograms	25
12	Maser threshold	26
13	Maxima and minima	27
14	Histogram for $r/A = 36, \varphi = 120^\circ, \nu = 0.15$	28
15	Steady state for $r/A = 6, \nu = 2$	29
16	Histograms: trapped/not trapped	32
17	OAM photon number, $r/A = 10, \nu = 0$	33
18	Histograms, damage after a pair	36
19	Emission probability after passage of a pair	38